Copy No. 114

CONFIDENTIAL

AMP Report 37.1R
AMG-NYU No. 49

STUDIES ON THE GAS BUBBLE RESULTING FROM UNDERWATER EXPLOSIONS

ON THE BEST LOCATION OF A MINE NEAR THE SEA BED

A Report Submitted
by the
Applied Mathematics Group, New York University
to the
Applied Mathematics Panel
National Defense Research Committee

CONFIDENTIAL

May 1944

DISTRIBUTION LIST

AMP Report 37.1R

No. of Copies	
24	Office of Executive Secretary, OSRD
20	Liaison Office, OSRD 1 - Admiralty Computing Service, John Todd 1 - Armament Research Dept., Branch for Theoretical Research, N. F. Mott 1 - Road Research Laboratory 1 - G. I. Taylor 1 - D. E. J. Offord 2 - B. S. Smith 1 - H. F. Willis and M. I. Willis 1 - H. N. V. Temperley 1 - S. Butterworth 1 - E. N. Fox
4	R. C. Tolman, Vice Chairman, NDRC
1	War Department Liaison Officer with NDRC Att: Col. H. C. Reuter
1	Coordinator of Research & Development, Navy Att: Lt. H. E. Wakelin
1	Office of the Chief of Ordnance, Technical Service Division Att: H. M. Morse
3	Aberdeen Proving Ground, Ordnance Research Center 1 - O. Veblen 1 - T. L. Smith
6	Chief of Bureau of Ordnance, Navy Department 1 - Lt. Comdr. S. Brunauer 1 - R. S. Burington 1 - R. J. Seeger 1 - A. Wertheimer
5	Director, David Taylor Model Basin 1 - Captain W. P. Roop 1 - G. E. Curl 1 - E. H. Kennard 1 - G. E. Hudson
2	Director, Naval Ordnance Laboratory
4	Chief, Bureau of Ships 1 - Lt. Comdr. R. W. Goranson 1 - Lt. J. E. Curtiss
1	AAF Proving Ground Command, Eglin Field, Fla. Att: Brig. Gen. Grandison Gardner
1	Research Group M Att: A. C. Olshem
1	J. E. Burchard, Chief, Division 2
4	J. T. Tate, Chief, Division 6 1 - W. C. Herring 1 - C. L. Pekeris
4	R. A. Connor, Chief, Division 8 2 - E. B. Wilson, Jr. 1 - P. M. Fye
1	Warren Weaver, Chief AMP
1	T. C. Fry
1	R. Courant
1	S. S. Wilks
1	E. J. Moulton
1	Garrett Birkhoff
1	J. G. Kirkwood
1	A. H. Taub
1	J. von Neumann
1	H. Weyl
1	M. Rees
1	I. S. Sokolnikoff

TABLE OF CONTENTS

TABLE OF GRAPHS

Studies on the Gas Bubble Resulting From Underwater Explosions

ON THE BEST LOCATION OF A MINE NEAR THE SEA BED

At the request of the David Taylor Model Basin of the Bureau of Ships and of Division Re 2 of the Bureau of Ordnance, a series of investigations has been undertaken by the New York University Group of the Applied Mathematics Panel of the N.D.R.C. with the object of analyzing the phenomena associated with the gas bubble produced by an underwater explosion.

The present study, carried out by Dr. Max Shiffman and Dr. Bernard Friedman, with the cooperation of the Mathematical Tables Project in the extensive numerical work, is concerned with the following problem: If a mine of given weight of explosive is to be placed near the sea bed, what position should it have to cause maximum damage to a target at the surface?

It seems appropriate to make a few introductory remarks about the broader research program of which this report is a part. Often the destructive effect of an underwater explosion is not wholly due to the high pressure shock of the explosion. After the initial shock wave has passed with enormous speed, a comparatively slow pulsation of the gas bubble (consisting of the burned gases) takes place. In the second and sometimes even third pulse of this motion of the bubble, a pressure pulse of considerable strength is emitted. While the peak of the shock pressure from the explosion is far above that of the later pulses (in typical cases, six to ten times the pressure of the second pulse), the duration of these later pulses is much longer (about twenty times as

long); so that the momentum imparted and the destruction caused may be comparable to that of the first shock. The importance of the second pulse has been confirmed more and more not only by model experiments, but also by analysis of actual damage to allied ships by mines [1], [2].*

Just as significant as the long duration of the second pressure pulse, is the migration of the gas bubble during the pulsation. The migration can increase the effect of the second pressure pulse because, under suitable conditions, the center of this pulse might be much closer to the target than the explosion. Factors influencing the motion of the bubble are: rigid walls such as the hull of a ship or the sea bed, which attract the bubble; the free surface of the water, which has a repulsive effect; and the buoyant force of gravity, which causes the bubble to rise towards the surface.

Understanding and controlling the complicated interplay of these effects is of sufficient practical importance to warrant comprehensive research. Unfortunately, a great variety of experiments with full size charges is hardly feasible, and experiments with small charges cannot easily be reinterpreted for large charges. Such difficulties call for theoretical investigation as a guide to experiment.

Historically, the earliest theoretical problem, satisfactorily analyzed in older studies, is that of a single spherical gas bubble immersed in an infinite body of water; in particular, the pressure as a function of time and distance, and the period of pulsation of the bubble can be explicitly determined.

For the past few years an extensive research program on underwater explosions has been pursued by G. I. Taylor

---

* Bracket references refer to the bibliography.

and his associates in England. In this country, theoretical work was started by C. Herring (Division 6, N.D.R.C.) and is being carried on at the David Taylor Model Basin (in particular by Captain W. P. Roop, E. H. Kennard, G. E. Hudson) and by the N.Y.U.Group of the A.M.P. at the request of the Model Basin and of the Bureau of Ordnance; considerable experimental research is being done at the Underwater Sound Laboratory of Division 8, N.D.R.C.

Taylor [3] and others have determined the upward motion of the bubble under the buoyant force of gravity, a motion taking place in jerks. Herring [4] and others have studied the manner in which rigid walls attract the bubble, assuming that the bubble is rather far from the wall. Shiffman [5] has developed an improved method which permits numerical analysis of the motion when the bubble is close to the wall, and even when it touches the wall. The influence of non-rigid walls and the repulsive effect of the free surface of the water on the bubble have also been studied. Much of the material is condensed and supplemented in the comprehensive work by Kennard[6].

A very important aspect of the problem is concerned with plastic-elastic deformations of the target in interaction with the motion of the water. The process of damage can be understood only by a careful analysis of this interaction. Extended research by J. G. Kirkwood [7] has established that the damage to a structure depends on the ratio of the duration time of the incoming pressure pulse to the "time constant" of the structure, i.e., the span of time during which the structure is "receptive" to the impinging pressure effects. If this ratio is small, the impulse is the more important factor for damage, while if it is large, the peak pressure is more important.

Another problem that should be mentioned is that of

the change in the shape of the gas bubble. The migrating gas bubble does not retain its spherical shape, but flattens out in a plane perpendicular to the direction of the motion. The result is a deceleration of the bubble and, as a consequence, an intensification of the pressure pulse. Preliminary studies of this effect have been carried out independently in England and at N.Y.U. by Dr. Shiffman [8].

Finally, the still unsolved problems presented by the striking phenomena occurring at the water surface must be mentioned. A proper interpretation of the "domes" and "plumes" rising into the air above the explosion should yield much information concerning the process taking place under water.

The effect of gravity in moving the bubble closer to the target is not the only factor which leads to increased damage by the second pulse. Another element of major importance, emphasized by Shiffman and Friedman, is that the peak pressure of the second pulse depends greatly on the state of motion of the bubble at the moment of the first contraction. It is shown that the peak pressure of the second pulse possesses a decided maximum if the gas bubble is stationary at the moment of contraction. For depths of water and weights of explosives actually used, it is indeed possible to keep the bubble stationary by counterbalancing the gravitational force with the attractive force of the sea bed and the repulsive force of the water surface.

This principle of stabilization forms the main point of the following report. It is assumed that the mine is to be placed fairly close to the sea bed, but not necessarily directly on it, and it is then found (roughly stated) that for mines of about 500 to 2000 lbs. of explosive in water about 70 to 150 ft. deep, the optimal position is about one

maximum bubble radius above the sea bed; this means that the mines should be moored approximately 20 ft. above the sea bed. More precisely, for water of given depth and for a mine of given weight of explosive, there is a definite optimum location for the detonation, that location being given by the principle of stabilization.

Of course, such a statement makes sense only if, at the outset, the position of the mine is restricted to a place deep under water, i.e., fairly distant from the target.

Similar problems concerning the optimal position of an explosion also occur for charges nearer the surface, and for charges dropped from fast flying planes and thus having an initial horizontal and vertical momentum at the instant of the detonation. The discussion of such questions is planned for later reports.

Richard Courant
Contractor's Technical Representative

Part 1. Discussion of the Results

1. Preliminary Remarks.

The present report is concerned with the following problem: what is the best location of a mine near the bottom of the sea so that during the secondary pulse the peak pressure is a maximum? The result obtained is: for weights of 500 to 2000 lbs. of T.N.T., in water of depth 100 to 150 ft., the mine should be placed about 20 ft. above the sea bed. More exact locations are contained in table 1, p. 9.

It is significant to compare different mine positions as to their effects on the secondary pulse. This report demonstrates that, during the secondary pulse, the highest possible peak pressure at the surface is obtained when the mine is placed in a definite "best" position. The theory indicates that if the mine is placed even a few feet away from its best location, the peak pressure might be as little as one-half of that corresponding to the "best" location.* Furthermore, when the mine is placed directly on the sea bed, experimental evidence is available showing that the secondary pulse is weak and erratic.[9]

Another point of interest is that the "best" position also increases the effectiveness of the shock wave compared with a location on the sea bed itself. In the latter case, some experiments indicate that the presence of the sea bed has no effect on the shock wave, and others, that it results in an increase of about 12 percent in the peak pressure and

---

* See the example discussed in section 4 below.

impulse.* On the other hand, when a mine is at the "best" location (about 20 ft. above the sea bed for a depth, say, of 100 ft.), then the shock wave peak pressure at the surface is increased about 25 percent over that of the sea bed position since the pressure at the surface is inversely proportional to the distance from the explosion.

2. The principle of stabilization.

The best location of the mine is determined by the following Principle of Stabilization: For a given mass of explosive, the maximum peak pressure in the secondary pulse is obtained if the gas bubble produced by the explosion is kept motionless at the time of its minimum size. This stabilization can be attained for mines by suitably balancing the upward buoyant force on the bubble against the downward attractive force due to the sea bed. In other cases, the repulsive force of the surface, as well as additional factors, could be utilized.

In part II, a mathematical demonstration of the principle of stabilization is given. The following plausible argument also points to the same result. In general, the total energy of the bubble and water is divided into two parts, namely, the kinetic energy of the water surrounding the bubble, and the internal energy of the gas inside the bubble. If the bubble is moving at the time of its minimum size, then some of the total energy is diverted into kinetic energy of the water and thus less is available for the internal energy

---

* [9] reports no change in the shock wave for a mud bottom. Experiments in Woods Hole for a sand bottom show an increase of 12 percent, according to an oral discussion. Theoretically, if the sea bed were perfectly rigid, the peak pressure would be multiplied by the factor $\sqrt[3]{2}$, which means an increase of 26 percent. Actually, however, the explosion tears a hole in the sea bed and also transmits a shock into it.

of the gas. This would reduce the pressure inside the gas and also the pressure in the water. To obtain the optimum pressure, therefore, this bubble must be motionless at the time of its minimum size.*

For an appraisal of the value of stabilization, the damage due to the secondary pulse must be studied. All theories of damage show that for a pressure pulse which lasts long relative to the time constant of the structure to be damaged, the damage is approximately proportional to the peak pressure and not to the impulse or energy. Since the duration of the secondary pulse is approximately twenty times that of the shock wave, it would seem that maximizing the peak pressure of the secondary pulse increases the damage.

3. The location of the mine.

Let W be the weight of the explosive in pounds, (the numerical values refer to T.N.T. for which the characteristic constants were available to the authors), D the distance in feet from the bottom of the sea to a point 33 feet above sea level (allowing for the pressure of the atmosphere), and B_o the distance in feet from the center of the mine to the sea bed. The problem is to determine the best value for B_o if W and D are given. This is more easily expressed in terms of the non-dimensional quantities which are used in part II. For the unit of length select

$$L = 13.2\left(\frac{W}{D}\right)^{1/3} \text{ ft.}, \tag{1.1}$$

which represents (approximately) the maximum radius of the

---

* This argument is not completely rigorous since contributions to the pressure in the water occur from the motion of the water as well as from the gas pressure inside the bubble. The fact that the gas pressure is the more important contribution arises from the mathematical analysis of the interplay of the two effects.

gas bubble at the first expansion. Set

$$(1.2) \qquad d = \frac{D}{L}\ ,\ b_o = \frac{B_o}{L}\ ,$$

so that d and b_o represent the distance D and B_o measured in "bubble radii".

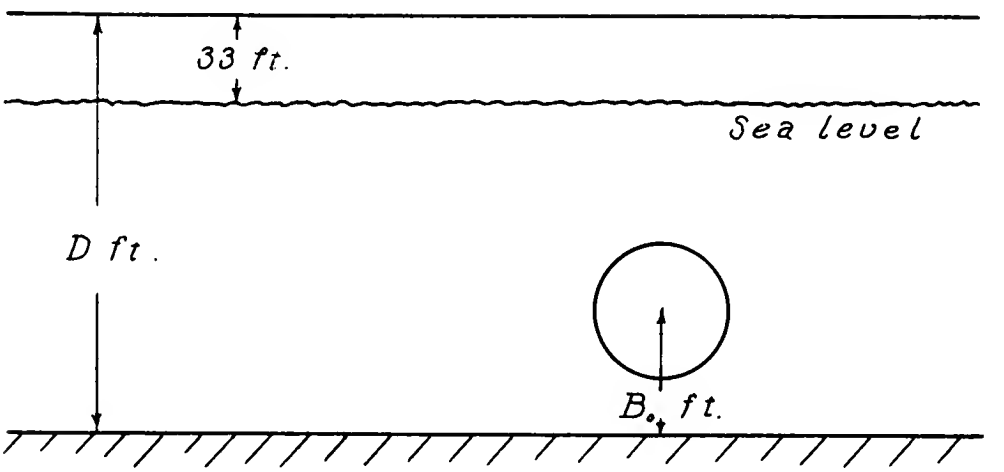

The best position of the mine is determined approximately from the equation

$$(1.3) \qquad d = 6.2b_o^2 + 3.3b_o + .4\ .$$

(See derivation in part III). Graphs of (1.1) and (1.3) are drawn in figures 1, 2 at the end.

On the basis of (1.1) and (1.3), the following table can be constructed showing the best location:

Table 1

Weight of T.N.T. (in lbs.)	Depth of Sea Bed From Sea Level (in ft.)	Best Location of Mine from Sea Bed (in ft.)
1500	150	21.0
1000	150	20.2
1000	100	17.0
500	100	15.5

The following limitations and qualifications should be noted. First, the effect of the free surface has been ignored, so that these results are valid if the mine is sufficiently far from the sea level, say, more than 3.5 L ft.* Second, it is assumed that the bubble does not meet the sea bed in the course of its motion. This is approximately equivalent to $B_o > .8L$. Third, the sea bed is assumed to act like a rigid wall.

The validity of this last assumption should be tested by experiment. But there are plausible reasons for supposing that as far as the balancing phenomenon is concerned, the sea bed does act very much like a rigid wall. During the largest part of the time of pulsation of the bubble, the bubble is large and the pressure in the water is low; therefore, a sand bottom could be considered as rigid. The balancing effect is determined in the main by this portion of the period of pulsation.

4. An example.

Consider a mine with 1500 lbs. of T.N.T, in water of depth 150 ft. Figure 3 is a graph showing the relative magnitudes of the peak pressure in the secondary pulse when the mine is placed at varying distances from the bottom of the sea. The best location of the mine is 21.0 ft. from the bottom; the resulting peak pressure at any point in the water, as computed in part II, is 2015/R atmospheres, where R is the distance in feet from the point to the center of the contracted bubble. If the mine is initially placed at any other distance from the bottom, this value for the peak pressure is to be multiplied by the factor whose graph is drawn in figure 3.

This graph demonstrates a remarkable sharpness** in the peak pressure curve as a function of the distance of the

---

* The correction due to the free surface is treated in part III, section 5.

** In reality the graph will not be quite as sharp because of deviations from the assumptions listed on page 12.

mine from the bottom. For example, if the mine is placed either 17 ft. or 29 ft. from the bottom, the peak pressure is only one-half of the maximum.

If one is interested in the damage to objects on the surface of the water, it is necessary to take into account the migration of the gas bubble. Again considering the above example, the peak pressure at the surface directly overhead is 15.6 atmospheres (excluding the reflection from the bottom) when the mine is placed 21.0 ft. from the bottom. For any other location of the mine, this value is to be multiplied by the factor whose graph is drawn in figure 4. The graph still exhibits a considerable sharpness, but if one places the mine somewhat higher than 21.0 ft. from the sea bed, the effect on the surface would be improved slightly. This is due to the upward migration of the bubble. Note, however, that if the mine is placed too high, say 27 ft. from the bottom, the favorable effect of the upward migration is sharply counterbalanced by the resulting weakness of the secondary pulse.

Part II. Mathematical Study of the Secondary Pressure Pulse

1. Introduction.

High pressure pulses are produced only when the size of the gas bubble is near its minimum. During this time, the buoyant force due to gravity is small. Likewise, the proximity of rigid walls or free surfaces will not materially affect the motion, since their influence depends on the ratio of the bubble radius to the distance from the bubble, and is small if this ratio is small. Therefore, during the stage of minimum size, the bubble can be considered as immersed in an infinite body of water and subject to no outside forces. The pressure pulse produced by the bubble under these

circumstances will be investigated.

On the other hand, all these outside influences do affect the bubble in the stage when it is not small. Consequently, in contracting to its minimum size, the bubble and surrounding water have a linear momentum which remains practically constant while the bubble passes through the minimum size stage when the outside influences can be neglected. The pressure pulse produced by the bubble depends on the linear momentum acquired by the bubble. The dependence of the peak pressure on this linear momentum is the main objective of this investigation and is represented in figure *b*.

For the derivation of this result, the following assumptions are made:

1. The water is an ideal incompressible fluid.
2. The bubble remains spherical in shape.
3. The gas inside the bubble is in thermal equilibrium at each instant and follows the adiabatic law.

These assumptions are reasonable for the major portion of the period of pulsation, and are violated only in the very short time interval when the radius of the bubble is small. The violations are in the nature of corrections to the theory, and will not materially affect the principle of stabilization. We shall not enter into a discussion of the assumptions, but merely refer to [4].

2. The Energy Equation.

Let A be the radius of the bubble at any time, B the vertical distance of its center from some horizontal level, and P_o the hydrostatic pressure of the water at the center of the bubble. The motion of the bubble is described by specifying A, B as functions of the time T.

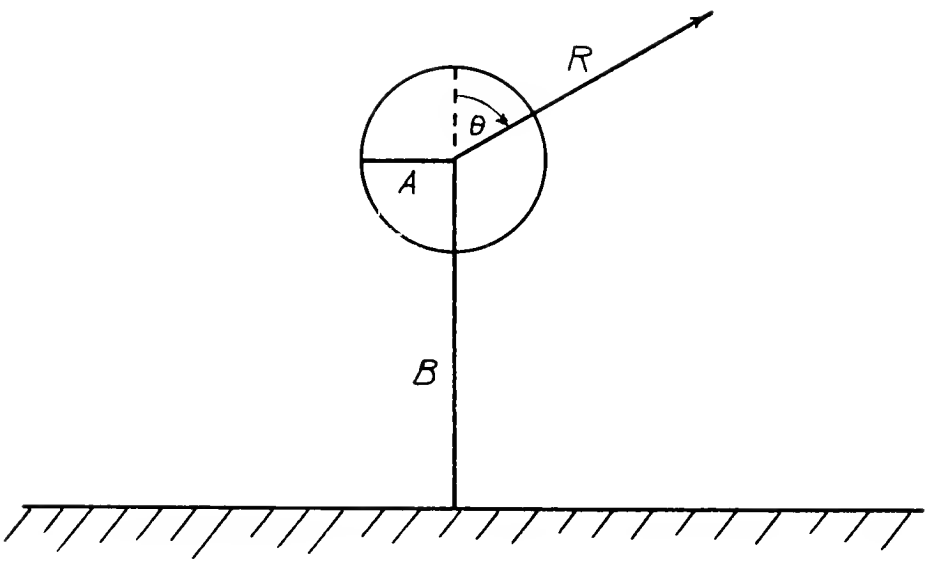

The velocity potential Φ describing the flow around a moving, pulsating sphere in an infinite body of water is easily obtained from classical hydrodynamics. It is

$$\Phi = \frac{A^2 A'}{R} + \frac{A^3 B'}{2} \frac{\cos\theta}{R^2} , \tag{2.1}$$

where R,θ are coordinates as indicated in the diagram above, and the "prime" denotes a time derivative. The kinetic energy $\mathcal{T}$ of the water is then

$$\mathcal{T} = 2\pi\rho A^3 [A'^2 + \frac{1}{6} B'^2] \tag{2.2}$$

where ρ is the density of the water. For these classical results, see, for example, [3] or Appendix II.

The potential energy $\mathcal{U}$ of the system of gas bubble and water is

$$\mathcal{U} = \frac{4}{3}\pi A^3 P_o + G(A) \tag{2.3}$$

where the first term is the gravitational potential energy

of the bubble due to the absence of water and the second term G(A) is the internal energy of the gas. If the gas obeys the adiabatic law, the internal energy is

$$G(A) = \frac{K M^{\gamma}}{A^{3(\gamma - 1)}}$$

where γ is the adiabatic exponent, K is a constant depending on the explosive, and M is the mass of the explosive used.

The energy equation is

$$\mathcal{T} + \mathcal{U} = E \tag{2.4}$$

where E is the constant total energy in the system (after the passage of the initial shock wave due to the explosion).

3. Non-dimensional variables.

A considerable simplification in the writing of the equations is obtained by introducing non-dimensional quantities with appropriate scaling factors. Likewise, in part III, it is even more important to introduce non-dimensional quantities. For the purpose of comparing the formulas developed in this part with those in part III, we shall use the scaling factors convenient for part III. It should be mentioned that these are not the most convenient factors to use if the results of part II were the sole objective.

Set

$$A = La, \quad B = Lb, \quad T = Ct, \tag{2.5}$$

where L,C are scaling factors with the dimensions of length, time, respectively, and a, b, t are non-dimensional variables. (Henceforth, capital letters will indicate dimensional quantities and small letters non-dimensional quantities.) The scaling factors

which we shall use are

$$(2.6) \qquad \begin{cases} L = \sqrt[3]{\dfrac{3E}{4\pi P_o}} \\ C = L\sqrt{\dfrac{3\rho}{2P_o}} \end{cases}$$

where P_o is the hydrostatic pressure at the center of the explosion, and ρ is the density of water.* These scaling factors are advantageous because they have a simple physical interpretation intimately connected with the motion of the bubble. It will be seen in part III that L is the maximum radius of the bubble if the internal energy of the gas could be neglected. Actually the maximum radius is approximately .92L. Also, it will be shown in part III that the time scaling factor C represents 2/3 of the period of pulsation of the bubble if no outside influences such as rigid walls or free surfaces are present.

The energy equation in terms of the non-dimensional variables becomes

$$(2.7) \qquad a^3\left[\dot{a}^2 + \frac{1}{6}\dot{b}^2\right] + a^3 + \frac{G(A)}{E} = 1,$$

where the "dot " denotes differentiation with respect to the non-dimensional time t.

4. The scaling factors and the internal energy of the gas for T. N. T.

It is desirable to express the scaling factors L,C in terms of the mass of explosive and the depth of the explosion.

---

* These scaling factors differ from those used by G. I. Taylor in [3].

Let D_o be the distance of the center of the explosion from a point 33 ft. above sea level, so that $P_o = \rho g D_o$. It is still necessary to express the energy constant E in terms of the mass of explosive. For the case of T. N. T., experimental results indicate that E is approximately one-half of the total chemical energy released by the explosion. See [4]. Slight changes in E will not materially affect the results since E appears in the form $\sqrt[3]{E}$. Using the values given by G. I. Taylor in [3], p. 4, and converting to the English system of measurements, one finds that

$$(2.8) \qquad \begin{cases} L = 13.2 \sqrt[3]{\dfrac{W}{D_o}} \text{ feet}, \\ \\ C = 2.85 \dfrac{W^{1/3}}{D_o^{5/6}} \text{ seconds}, \end{cases}$$

where W is the weight of T. N. T. in pounds, and D_o is the distance in feet of the center of the explosion from a point 33 ft. above sea level.

Likewise, making use of the experimental values given by G. I. Taylor in [3], p. 4, the quantity $\frac{G(A)}{E}$ for T. N. T. is, in metric units,

$$\frac{G(A)}{E} = \frac{1.183 M_{gr}^{1/4}}{A^{3/4}},$$

where M_{gr} is the mass of T. N. T. in grams. Changing to non-dimensional variables, one obtains

$$(2.9) \qquad \frac{G(A)}{E} = \frac{k}{a^{3/4}}$$

where $k = \dfrac{1.183 M_{gr}^{1/4}}{L_{cm}^{3/4}}$.

Changing to English units and using (2.8), one finds that

$$k = .0607\, D_o^{1/4} \quad , \tag{2.10}$$

where D_o has the same meaning as in (2.8). Equations (2.9) and (2.10) are the desired expressions of the internal energy for T.N.T.

5. The equations of motion for small values of the radius a.

The secondary high pressure pulse is emitted when the bubble is near its minimum size, and henceforth we shall consider the case when the radius is small. The additive term a^3 in the energy equation (2.7) is then negligible compared with the number 1, and the energy equation becomes

$$a^3(\dot{a}^2 + \frac{1}{6}\dot{b}^2) + \frac{k}{a^{3/4}} = 1. \tag{2.11}$$

The Lagrangean equations of motion are

$$\frac{d}{dt}\frac{\partial \mathcal{L}}{\partial \dot{a}} - \frac{\partial \mathcal{L}}{\partial a} = 0 \tag{2.12}$$

$$\frac{d}{dt}\frac{\partial \mathcal{L}}{\partial \dot{b}} - \frac{\partial \mathcal{L}}{\partial b} = 0 \tag{2.13}$$

where $\mathcal{L} = \mathcal{T} - \mathcal{U}$. They become

$$\frac{d}{dt}(2\, a^3\dot{a}) = 3a^2(\dot{a}^2 + \frac{1}{6}\dot{b}^2) + \frac{3}{4}\frac{k}{a^{7/4}} \quad , \tag{2.14}$$

$$\frac{d}{dt}(\frac{1}{3}\, a^3\, \dot{b}) = 0. \tag{2.15}$$

The equation (2.15) shows that when the bubble is near its minimum size, the linear momentum $\frac{1}{3} a^3 \dot{b}$ remains constant. Denote this constant value by $\bar{s}$. Then

$$\dot{b} = \frac{3\bar{s}}{a^3} \quad , \tag{2.16}$$

and the energy equation (2.11) yields

$$\dot{a}^2 = \frac{1}{a^3} - \frac{k}{a^{15/4}} - \frac{3\bar{s}^2}{2a^6} \quad . \tag{2.17}$$

The equations (2.16), (2.17) completely determine, in terms of $\bar{s}$, the motion of the bubble during its most interesting phase when the radius a is small. An integration of (2.17) and then of (2.16), yields a, b as functions of t.

Equation (2.14) gives an expression for the quantity $(a^2\dot{a})^{\cdot}$, which is important for the determination of the pressure:

$$(a^2\dot{a})^{\cdot} = a\left(\frac{1}{2}\dot{a}^2 + \frac{1}{4}\dot{b}^2 + \frac{3}{8}\frac{k}{a^{15/4}} \right) \quad . \tag{2.18}$$

Substituting (2.16), (2.17) in (2.18), we obtain

$$(a^2\dot{a})^{\cdot} = \frac{1}{2a^2} + \frac{3\bar{s}^2}{2a^5} - \frac{k}{8a^{11/4}} \quad . \tag{2.19}$$

6. <u>The minimum radius.</u>

The value of a quantity q at the time when the bubble is exactly at its minimum size will be denoted by $\bar{q}$. The minimum radius $\bar{a}$ of the bubble is obtained by setting $\dot{a} = 0$ in (2.17). The resulting equation is simplified by introducing, in place of $\bar{a}$, the (non-dimensional) internal energy

$\bar{u}$ of the gas, defined by

$$(2.20) \qquad \bar{u} = \frac{k}{\bar{a}^{3/4}} \text{ , or } \bar{a} = \left(\frac{k}{\bar{u}}\right)^{4/3} .$$

The quantity $\bar{u}$ represents the portion of the total energy of the system which exists as internal energy of the gas at the time of minimum size. From (2.17), we get the following equation which determines $\bar{u}$:

$$(2.21) \qquad \frac{1 - \bar{u}}{\bar{u}^4} = \frac{3}{2}\left(\frac{\bar{s}}{k^2}\right)^2 , \text{ (Graphed in Fig. 5).}$$

The values of various other quantities at the time of minimum size of the bubble are of interest. From (2.16) we have

$$(2.22) \qquad \bar{\dot{b}} = \frac{3\bar{s}}{\bar{a}^3} = \frac{3\bar{s}}{k^4}\bar{u}^4 ,$$

and (2.19) yields

$$(2.23) \qquad \overline{(a^2\dot{a})^{\cdot}} = \frac{3}{8k^{8/3}}\bar{u}^{8/3}(4 - 3\bar{u}) .$$

Thus, given $\bar{s}$, the internal energy $\bar{u}$ at minimum size is obtained from equation (2.21). All the other quantities $\bar{a}$, $\bar{\dot{b}}$, $\overline{(a^2\dot{a})^{\cdot}}$ can then be found from (2.20), (2.22), (2.23).

7. The pressure pulse.

Sections 5 and 6 give a complete description of the motion of the bubble when it is near its minimum size. We shall now investigate the pressure pulse delivered to the surrounding water.

The potential function Φ for the flow of the surrounding water has been constructed in equation (2.1). The pressure in the water can be obtained from Bernoulli's equation as follows:

$$(2.24) \qquad \frac{P}{\rho} + \frac{1}{2} (\text{grad } \Phi)^2 - \left(\frac{\partial \Phi}{\partial T} - B' \frac{\partial \Phi}{\partial Z}\right) = 0,$$

where P is the excess over hydrostatic pressure, $Z = R \cos \theta$, and the term $B' \frac{\partial \Phi}{\partial Z}$ appears because of the moving coordinate system. A substitution of (2.1) in (2.24) yields

$$(2.25) \qquad \frac{P}{\rho} = \frac{(A^2 A')'}{R} + \text{terms in higher powers of } \frac{1}{R}.$$

For points in water not too near the bubble, the first term on the right hand side of (2.25) is dominant and the other terms may be dropped. Introducing non-dimensional variables, we obtain

$$(2.26) \qquad P = \frac{L^3}{C^2} \frac{(a^2 \dot{a})^{\cdot}}{R} = \frac{2P_0}{3} \cdot \frac{L}{R} (a^2 \dot{a})^{\cdot}.$$

The pressure in the water, therefore, depends essentially on the quantity $(a^2 \dot{a})^{\cdot}$.

The formula (2.18) for $(a^2 \dot{a})^{\cdot}$ can be given an interesting interpretation. The last term $\frac{3}{8} \frac{k}{a^{15/4}}$ represents the (non-dimensional) pressure of the gas inside the bubble, and (2.26) then shows that the pressure at any point in the water is composed of two parts: the internal pressure of the gas, and the dynamic pressure due to the motion of the water. This is more clearly seen if equations (2.26), (2.18) are rewritten in terms of the original dimensional variables. The

result is

$$(2.27) \qquad P = \frac{A}{R}\left(\frac{1}{2}\rho A'^2 + \frac{1}{4}\rho B'^2 + p(A)\right) \quad ,$$

where $p(A)$ is the pressure of the gas inside the bubble when its radius is A.

The principle of stabilization asserts that the most important term in the expression (2.27) is the gas pressure term $p(A)$. To obtain the maximum possible effect, one should maximize $p(A)$ even at the expense of complete elimination of the dynamic terms $\frac{1}{2}\rho A'^2 + \frac{1}{4}\rho B'^2$. This is not obvious and requires a mathematical proof.

Returning now to the expression (2.26) for P, we wish to determine the time when the pressure pulse reaches a peak value. It is to be expected that the peak pressure occurs when the bubble is of minimum size. Although this is not obvious from the expression (2.18) for $(a^2\dot{a})^{\cdot}$, it is a simple consequence of the equation (2.19). By differentiating (2.19) with respect to a and by using (2.17), we have

$$\frac{d}{da}(a^2\dot{a})^{\cdot} = -\frac{1}{a^3} - \frac{15}{2}\frac{\bar{s}^2}{a^6} + \frac{11}{32}\frac{k}{a^{15/4}} = -\dot{a}^2 - \frac{9\bar{s}^2}{a^6} - \frac{21}{32}\frac{k}{a^{15/4}} \cdot$$

This shows that $\frac{d}{da}(a^2\dot{a})^{\cdot}$ is negative and therefore attains its maximum at the smallest possible value of a. Hence the peak pressure occurs at the time of the minimum size of the bubble.

The value of the peak pressure $\bar{P}$ can now be obtained by substituting (2.23) in (2.26); the resulting expression is

$$(2.28) \qquad \bar{P} = \frac{1}{R} \cdot \frac{P_o L}{4k^{8/3}} \cdot \bar{u}^{8/3}(4 - 3\bar{u}) \cdot$$

This indicates the dependence of the peak pressure $\bar{P}$ on the internal energy $\bar{u}$ at the time of minimum size, and through (2.21), on the linear momentum $\bar{s}$.

The quantity $\bar{u}^{8/3}(4 - 3\bar{u})$ will be called the "pressure factor" and will be denoted by the symbol $\bar{q}$:

$$\bar{q} = \bar{u}^{8/3}(4 - 3\bar{u}) \cdot \tag{2.29}$$

It depends on $\bar{s}$ by virtue of (2.21).

8. The optimum peak pressure.

We are now in a position to find that linear momentum $\bar{s}$ which produces the maximum peak pressure. The peak pressure $\bar{P}$, by (2.28), is proportional to the pressure factor $\bar{q}$ in (2.29), which in turn depends on $\bar{s}$ by virtue of (2.21). A graph of $\bar{q}$ as a function of $\frac{\bar{s}}{k^2}$ is drawn in figure 6, and demonstrates the very significant fact that $\bar{q}$ is largest when $\bar{s}$ is practically 0 (or $\bar{u}$ practically 1). Actually, by (2.29), $\bar{q}$ is a maximum when $\bar{u} = \frac{32}{33}$, or by (2.21), when $\bar{s} = .151\ k^2$. But since k is small, this differs so little from $\bar{s} = 0$ that it can be neglected. See figure 6.

Thus, the following general Principle of Stabilization has been demonstrated: For a given mass of explosive, the optimum peak pressure in the secondary pulse is obtained by keeping the bubble motionless at the time of its minimum size.

The value of the optimum peak pressure $\bar{P}_{opt.}$ can be obtained from (2.28) by setting $\bar{u} = 1$, with the result

$$\bar{P}_{opt.} = \frac{1}{R} \cdot \frac{P_o L}{4k^{8/3}} \cdot$$

Using (2.7) and (2.10), and expressing P_o in atmospheres by means of $P_o = D_o/33$ atmospheres, where D_o is the distance in feet of the center of the explosion from a point

33 ft. above sea level, we have

$$\bar{P}_{opt.} = 176 \frac{W^{1/3}}{R} \text{ atmospheres} \tag{2.30}$$

where W is the weight of T. N. T. in pounds and R is the distance from the center of the bubble in feet.

This may be compared with the peak pressure of the primary shock wave, whose value, experimentally obtained, is*

$$P_{shock} = 1160 \frac{W^{1/3}}{R} \text{ atmospheres.}$$

The optimum peak pressure of the secondary pulse is approximately 15 percent of the shock wave peak pressure, but the duration is much longer, as will be seen in the next section.

9. The impulse.

The impulse I per unit area, carried by the secondary pulse, is the time integral of the pressure,

$$I = \int P dT = C \int P dt,$$

where the limits of integration are the times when $P = 0$.** By (2.26),

$$I = \frac{2P_o C}{3} \cdot \frac{L}{R} \int (a^2 \dot{a})^{\cdot} dt,$$

where the limits of integration are the times when $(a^2\dot{a})^{\cdot} = 0$. Using the fact that the motion is approximately symmetric about

---

* See [3] page 13, where this experimental result is quoted in metric units.

** The significance of this value of the impulse will be discussed later.

the time of the minimum size of the bubble, the above integral becomes

$$(2.31) \qquad I = \frac{4P_o C}{3} \cdot \frac{L}{R} \cdot [a^{2\dot{}}\dot{a}],$$

where $[a^{2\dot{}}\dot{a}]$ is to be evaluated at the time when $(a^{2\dot{}}\dot{a})^{\cdot} = 0$, or $a^{2\dot{}}\dot{a}$ is a maximum.

Equations (2.8), (2.9) and (2.16) yield

$$a^{4\dot{}2} = a - ka^{1/4} - \frac{3\bar{s}^2}{2a^2} - a^4$$

and

$$\frac{d}{da}(a^{4\dot{}2}) = 1 - \frac{k}{4a^{3/4}} + \frac{3\bar{s}^2}{a^3} - 4a^3 .$$

Setting the last expression equal to zero in order to find the maximum of $(a^{2\dot{}}\dot{a})^2$, we obtain an equation for a. If both k and $\bar{s}$ were equal to zero, the solution of this equation would be $a = .63$. In a more realistic case when $k = .2$, $\bar{s} = .06$, one obtains $a = .61$. This illustrates that the value of a when $a^{2\dot{}}\dot{a}$ is a maximum is not very sensitive to changes in the momentum $\bar{s}$, since $\bar{s}$ is generally quite small in actual cases.* Using $a = .61$ and $k = .2$, the value of $[a^{2\dot{}}\dot{a}]$ is .55.

By (2.7), equation (2.31) becomes

$$I = .73 \frac{P_o CL}{R} = \frac{.83}{D_o^{1/6}} \frac{W^{2/3}}{R} \text{ atmosphere-seconds.}$$

Taking a typical case of a depth of 100 ft., so that $D_o = 133$, we find that

$$(2.32) \qquad I = .37 \frac{W^{2/3}}{R} \text{ atmosphere-seconds.}$$

---

* See Part III.

We have shown that the impulse carried by the secondary pulse is practically independent of the linear momentum $\bar{s}$ of the bubble, and is given by (2.32).

The impulse carried by the primary shock wave is experimentally measured to be*

$$I_{shock} = .12 \frac{W^{2/3}}{R} \text{ atmosphere-seconds.}$$

A comparison with (2.32) indicates that the impulse carried by the secondary pulse is three times the impulse carried by the shock wave.

This conclusion can be stated in an approximate manner in terms of the durations of the pulses. Using the relation between the peak pressures obtained at the end of the last section, one can state that the secondary pulse lasts about eighteen times as long as the shock wave.

This result, and formula (2.32), should not be taken too literally but merely as order of magnitude statements. The reason for this is that the impulse carried by the secondary pulse was computed between the times when the pressure is zero. This includes a relatively long period of time during which the pressure is low, and the resulting contribution to the impulse will not be experimentally noticed and will not have much effect in damaging structures.

---

* [3], p.13

Part III. The Mechanism of Stabilization by Gravity and the Sea Bed.

1. The exact equations of motion.

In this part, the effects of gravity and of a rigid wall upon the motion of the bubble are considered. The linear momentum $\bar{s}$ produced by these factors in the course of one complete pulsation of the bubble is calculated. As was shown in part II, it is $\bar{s}$ which determines the peak pressure produced by the bubble at the time of its minimum size. An equation for determining the best location of the mine can be obtained by setting the momentum $\bar{s}$ equal to zero.

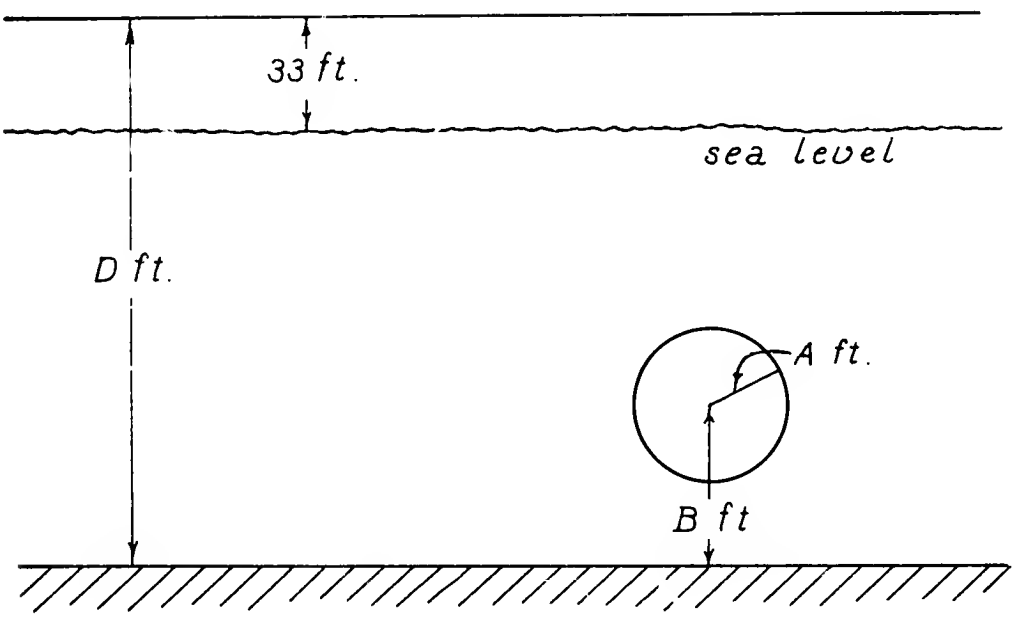

Use the same variables A,B as in part II and let D stand for the (fixed) distance of the sea bed from a point 33 ft. above sea level. In place of the equations (2.2), (2.3), (2.4), we have*

$$(3.1)\qquad 2\pi\rho A^3\left[(1+f_o)\dot{A}^2 - 2f_1\ddot{A}\dot{B} + (\tfrac{1}{6}+f_2)\dot{B}^2\right]$$

$$+\frac{4}{3}\pi A^3\rho g(D-B) + G(A) = E,$$

where f_o, f_1, f_2 are functions of the ratio A/B which represent the influence of the rigid wall on the motion of the bubble, $\frac{4}{3}\pi A^3\rho g(D-B)$ represents the gravitational potential energy due to the lack of water in the space occupied by the bubble, and g is the acceleration due to gravity. Explicit expressions for f_o, f_1, f_2 are derived in [5], and will be reproduced in appendix II of this report.

Introduce non-dimensional quantities as in equations (2.5), (2.6) of part II, sections 3 and 4. The energy equation becomes

$$(3.2)\qquad a^3[(1+f_o)\dot{a}^2 - 2f_1\ddot{a}\dot{b} + (\tfrac{1}{6}+f_2)\dot{b}^2]$$

$$+\frac{d-b}{d-b_o}a^3 + \frac{k}{a^{3/4}} = 1,$$

where $d = \frac{D}{L}$, $b_o = \frac{B_o}{L}$ and B_o is the initial distance of the bubble from the sea bed.

The motion of the bubble is determined from (3.2) and one of the Lagrangean equations (2.12), (2.13). Using

---

* See appendix II for details.

the b-equation (2.13), we obtain

$$(3.3)\qquad \frac{d}{dt}\left[2a^3\left(\frac{1}{6}+f_2\right)\dot{b} - 2a^3 f_1 \dot{a}\right]$$

$$= -\frac{a^4}{2b^2}\left[\frac{df_o}{d\alpha}\dot{a}^2 - 2\frac{df_1}{d\alpha}\ddot{ab} + \frac{df_2}{d\alpha}\dot{b}^2\right] + \frac{1}{d-b_o}a^3,$$

where

$$(3.4)\qquad \alpha = \frac{a}{2b},$$

and the quantities f_o, f_1, f_2 are functions of α only.

The differential equations (3.2), (3.3) are to be integrated, subject to the following initial condition:

$$\text{at } t = 0, \quad a = a_o, \ \dot{a} = 0$$

$$b = b_o, \ \dot{b} = 0,$$

where a_o is the smallest root (near $k^{4/3}$) of $a^3 + \frac{k}{a^{3/4}} = 1$. Of course, these initial conditions are not exactly realistic, since at the very beginning a shock wave is formed by the explosion. But the time interval required for incompressible flow to set in is relatively minute and may be ignored.*

The quantity in the brackets on the left-hand side of (3.3) is the linear momentum s of the system. The first term on the right-hand side of (3.3) is due to the presence of the rigid wall, and the second term is due to gravity.

By integrating equation (3.3) we obtain the momentum $\bar{s}$ at the end of the period of pulsation of the bubble:

---

* See [4].

$$(3.5)\quad \bar{s} = -\int_o^{\bar{t}} \frac{a^4}{2b^2}\left[\frac{df_o}{d\alpha}\dot{a}^2 - 2\frac{df_1}{d\alpha}\dot{a}\dot{b} + \frac{df_2}{d\alpha}\dot{b}^2\right] dt$$

$$+ \frac{1}{d-b_o}\int_o^{\bar{t}} a^3 dt\ ,$$

where the integration is extended over the full period $\bar{t}$ of the pulsation, from the explosion to the time of minimum size.

2. The approximate evaluation of the period and the momentum.

The results of a numerical integration of equations (3.2), (3.3) are tabulated for special cases in appendix II. They serve as a check on the approximations which will now be made to evaluate the period $\bar{t}$ and the momentum $\bar{s}$.

The bubble expands to a maximum size before contracting again. Indicate the value of a quantity at the time of maximum size by a subscript 1. Thus t_1 is the time of maximum size, s_1 is the linear momentum, etc. We shall introduce the following approximations which are especially accurate when the bubble is in its balanced position:

1. The time $\bar{t}$ and linear momentum $\bar{s}$ at the minimum size of the bubble is twice the corresponding quantity at the maximum size; i. e., $\bar{t} = 2t_1$, $\bar{s} = 2s_1$. This assumption agrees very closely with the numerical integration of the equations. It means that the motion is approximately symmetric about the time t_1 of maximum size. This would be exactly correct if the b-coordinate did not vary.

2. During the first half of the period of pulsation, until time t_1, $\dot{b}$ is small and can be taken as zero, so that b remains equal to b_o. This agrees satisfactorily with the numerical integration, as well as with experimental evidence.

Substituting $b = b_o$ in (3.2), we get

$$\mathring{a} = \frac{\sqrt{1 - a^3 - k a^{-3/4}}}{a^{3/2}\sqrt{1 + f_o}} \quad . \tag{3.6}$$

The solution of (3.6) is immediately obtained by integration, with the following result for the half-period t_1:

$$t_1 = \int_o^{t_1} dt = \int_{a_o}^{a_1} \frac{a^{3/2}\sqrt{1 + f_o}}{\sqrt{1 - a^3 - k a^{-3/4}}}\, da \tag{3.7}$$

where a_o is the smallest and a_1 the largest root of

$$1 - a^3 - k a^{-3/4} = 0. \tag{3.8}$$

To evaluate the integral (3.7) it is necessary to have a specific value for k. The value of k is given by (2.10) and depends on the distance D_o of the explosion from a point 33 ft. above sea level. The following table is calculated from (2.10):

D_o	33	83	133	183
k	.146	.183	.206	.223

Selecting a depth of water of about 100 ft. as typical, the value of k is approximately .2. We shall select this value of k throughout the remaining calculations. A different value for k will change the formulas slightly.

For $k = .2$, the roots a_o, a_1 of (3.8) are

$$a_o = .118, \qquad a_1 = .924. \tag{3.9}$$

The last equation (3.9) is noteworthy, since a_1 represents the non-dimensional maximum radius of the bubble. The actual maximum radius A_1 is thus

$$A_1 = .924\ L.$$

If the internal energy $\frac{k}{a^{3/4}}$ of the gas were neglected, the maximum radius would be exactly L.

The quantity $\sqrt{1 + f_o}$ in the integral (3.7) is very closely equal to $1 + \frac{\alpha}{2} = 1 + \frac{a}{4b_o}$ as is shown in appendix II. Making this approximation, we can evaluate the integral (3.7) numerically. This numerical evaluation is discussed in appendix III, the result being

$$t_1 = .735 + \frac{.136}{b_o} .$$

The total (non-dimensional) period $\bar{t}$ of the pulsation is therefore

$$(3.10) \qquad \bar{t} = 2t_1 = 1.47 + \frac{.272}{b_o} = 1.47 \left(1 + \frac{.185}{b_o}\right) .$$

Formula (3.10) shows that if no rigid walls are present $(b_o = \infty)$, the actual period $\bar{T}$ in seconds would be

$$\bar{T} = 1.47\ C,$$

or about 3/2 times C. This provides the physical interpretation of the scaling factor C mentioned in section 3 of part II.

Substituting $b = b_o$, $\dot{b} = 0$ in (3.5), we obtain for

the half-momentum s_1,

$$s_1 = - \int_o^{t_1} \frac{a^4}{2b_o^2} \frac{df_o}{d\alpha} \dot{a}^2 dt + \frac{1}{d-b_o} \int_o^{t_1} a^3 dt,$$

or

$$(3.11)\quad s_1 = - \frac{1}{2b_o^2} \int_{a_o}^{a_1} \frac{a^{5/2} \sqrt{1 - a^3 - ka^{-3/4}} \cdot \frac{df_o}{d\alpha}}{\sqrt{1 + f_o}} da$$

$$+ \frac{1}{d-b_o} \int_{a_o}^{a_1} \frac{a^{9/2} \sqrt{1 + f_o}}{\sqrt{1 - a^3 - ka^{-3/4}}} da ,$$

using (3.6). The first term on the right hand side of (3.11) is the downward momentum due to the rigid wall, and the second term is the upward momentum due to gravity.

Again taking $k = .2$, using the approximation $\sqrt{1 + f_o} = 1 + \frac{a}{4b_o}$, $\frac{df_o/d\alpha}{\sqrt{1 + f_o}} = 1 - \frac{a}{4b_o}$, and evaluating these integrals numerically, we get the following expression for the full momentum $\bar{s}$:

$$(3.12)\quad \bar{s} = - \left(\frac{.113}{b_o^2} - \frac{.019}{b_o^3} \right) + \frac{1}{d-b_o} \left(.704 + \frac{.148}{b_o} \right).$$

See appendix III for the numerical evaluations.

3. <u>The stabilized position</u>.

By the principle of stabilization, the maximum peak

pressure is obtained by setting $\bar{s} = 0$, with the result

$$d - b_o = \frac{.704 + \frac{.148}{b_o}}{\frac{.113}{b_o^2} - \frac{.019}{b_o^3}} \quad .$$

Expressing d in descending powers of b_o, we get

$$(3.13) \qquad d = 6.2\, b_o^2 + 3.3\, b_o + .4 \quad .$$

A graph of equation (3.13) is drawn in figure 2.

More generally, the peak pressure, as a function of the distance b_o of the mine from the sea bottom, is obtained by combining equation (2.28), (2.29), figure 6, and equation (3.12). As a typical example of this dependence, consider the case discussed in section 3, part I, of a mine containing 1500 lbs. of T. N. T. in water of depth 150 ft. The scaling factor L, as obtained from figure 1, is

$$L = 27.6 \text{ ft.}$$

The depth D of the sea bed from a point 33 ft. above sea level is 183 ft., so that

$$d = \frac{D}{L} = 6.63.$$

The best location of the mine according to figure 2 is $b_o = .76$, or

$$B_o = Lb_o = 21 \text{ ft.}$$

above the sea bed.

If the mine is located at various other distances B_o, the pressure factor $\bar{q}$ can be obtained from figure 6 by first determining $\bar{s}$ from equation (3.12). The results are tabulated below, and the graph is drawn in figure 3.

b_o	.6	.7	.76	.8	.9	1.0	1.1	1.2
$\bar{s}$	-.066	-.020	+.003	.015	.039	.059	.074	.087
$\bar{q}$	.51	.92	1.0	.96	.72	.55	.47	.42

As stated in section 3, part I, figure 3 shows a remarkable sharpness in the peak pressure curve as a function of the distance from the bottom.

4. The migration of the bubble.

A formula for the distance travelled by the bubble in the course of its pulsation is difficult to obtain because it involves a complicated repeated integration. But by combining a theoretical argument with the results of numerical integration, an empirical formula can be developed.

It seems reasonable to suppose that the displacement $\Delta b = \bar{b} - b_o$ of the bubble is an odd function of $\bar{s}$. It can therefore be represented by the beginning terms of a Taylor expansion,

$$\Delta b = c_1 \bar{s} + c_2 \bar{s}^3 ,$$

where c_1, c_2 are appropriate constants. In fact, a theoretical justification of this can be given on the basis of the differential equations (3.2), (3.3), but this will be omitted here.

We can determine the constants c_1, c_2 empirically by using the results of the numerical integration tabulated in

appendix I. The least squares solution yields the following formula:

$$\Delta b = 19\bar{s} \left(1 - 62\bar{s}^{-2}\right). \tag{3.14}$$

A graph of (3.14) is drawn in figure 7, and is compared with the tabulated values. The formula (3.14) is seen to be very close to the tabulations.

5. The correction due to the free surface.

For the sake of completeness, we shall include some remarks concerning the effect of the free water surface. The latter exerts a repellent force on the bubble, aiding the downward force of the sea bed. A complete discussion would require a knowledge of the potential function Φ and of the corresponding values for f_o, f_1 and f_2. A careful examination of the previous argument, however, shows that only the first terms in the expansions of f_o and $\frac{\partial f_o}{\partial b}$ in powers of a were used. In appendix II these first terms are obtained by successive reflections. The results are as follows:

If C is the depth of the bubble below the free surface, and x is set equal to $\frac{C-B}{C+B}$, then the expansion of f_o begins with

$$\frac{a}{2b} F(x)$$

and the expansion of $\frac{\partial f_o}{\partial b}$ begins with

$$- \frac{a}{2b^2} G(x)$$

where the formulas for $F(x)$ and $G(x)$ are given in appendix II. A short table of their values follows:

x	1	.9	.8	.7	.6	.5	.4	.3	.2	.1	0
F(x)	1	.86	.72	.58	.43	.28	.11	-.06	-.25	-.46	-.69
G(x)	1	1.00	1.00	1.01	1.03	1.07	1.10	1.22	1.33	1.54	1.86

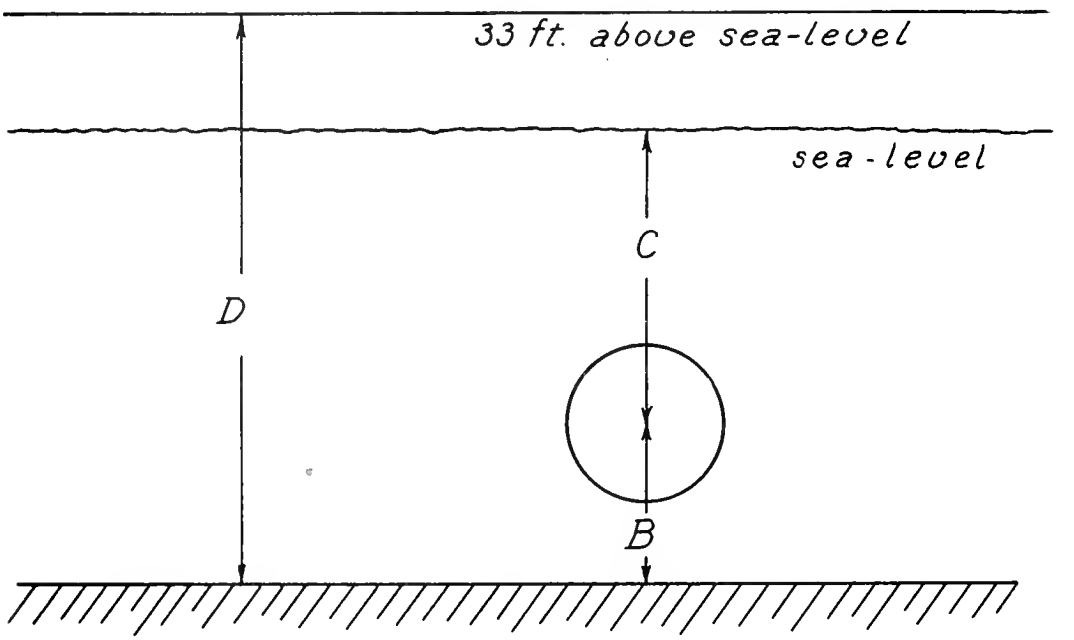

When these expansions are used, formulas (3.10) and (3.12) for $\bar{t}$ and $\bar{s}$ are modified, as follows:

$$\bar{t} = 1.47 \left(1 + \frac{.185\ F(x)}{b_o} \right) \tag{3.15}$$

$$\bar{s} = - \frac{G(x)}{b_o^2} \left(.113 - \frac{.019\ F(x)}{b_o} \right) + \frac{1}{d-b_o} \left(.704 + \frac{.148\ F(x)}{b_o} \right) . \tag{3.16}$$

It is to be noted that $x = 1$ corresponds to no free surface ($C = \infty$), while $x = 0$ corresponds to a point midway between the free surface and the rigid bottom.

An interesting result is that $F(x) = 0$ when $x = 1/3$, so that the influence of the free surface on the period of the bubble cancels the influence of the rigid bottom.

Appendix I. The Numerical Integration of the Differential Equations.

To test the validity of the approximations made in part III, the exact differential equations (3.2), (3.3) were integrated numerically. The coefficients f_o, f_1, f_2 and their derivatives with respect to α, are tabulated in table 4, appendix II. The numerical integration was carried out by the Mathematical Tables Project operating under the Applied Mathematics Panel.*

In this report we have not reproduced the complete tables, but have included the graphs drawn in figures 8 - 11, which are based on these tables. Here we shall set down only the most interesting items in these calculations, namely, the behavior at the beginning, at the time of maximum size, and at the time of minimum size.** The following table shows the results:

---

* In particular, Dr. G. Blanche, Dr. C. Lanczos and Dr. A. N. Lowan helped overcome the considerable difficulties in the numerical integration.

** Details of the computation can be obtained from an extensive report by the Mathematical Tables Project prepared for the Applied Mathematics Panel.

Table 2. The results of numerical integration

	t	a	$\dot{a}$	b	$\dot{b}$	s	$\dot{s}$
I. d = 11.17 b_o = 1.5	0	.1172	0	1.5	0	0	.00017
	.8289	.925	0	1.565	.066	.0189	.079
	1.657	.192	0	2.11	16.0	.0378	.0006
2. d = 11.17 b_o = 1.17	0	.1172	0	1.17	0	0	.00016
	.8505	.926	0	1.243	.0231	.00716	.0794
	1.6993	.138	0	1.49	15.8	.0139	.0
3. d = 11.17 b_o = 1.08	0	.1172	0	1.08	0	0	0
	.8576	.926	0	1.156	.006	.00205	.0791
	1.7146	.120	0	1.19	6.9	.00393	0
4. d = 11.17 b_o = .9	0	.1172	0	.9	0	0	0
	.8753	.926	0	.986	-.041	-.0154	.0769
	1.7574	.167	0	.352	-16.9	-.0270	-.076
5. d = ∞* b_o = 2.0	0	.117	0	2.0	0	0	0
	.8043	.922	0	2.01	-.0470	-.0127	-.0001
	1.610	.163	0	1.58	-17.4	-.0251	-.00236
6. d = ∞* b_o = 1.5	0	.117	0	1.5	0	0	0
	.8204	.923	0	1.52	- .0769	-.0219	-.0002
	1.6504	.202	0	.808	-15.4	-.0426	-.007
7. d = ∞* b_o = 1.2	0	.117	0	1.2	0	0	0
	.8266	.922	0	1.23	- .111	-.0339	-.0004
	1.699	.237	0	.282	-12.6	-.0645	-.58

* This case corresponds to a rigid wall alone, with gravity ignored.

The period $\bar{t}$ and the momentum $\bar{s}$ for the cases listed above were computed from the formulas developed in part III. They are collected in the following table, and compared with the numerical values given in the preceding table. The agreement is excellent.

TABLE 3.

	$\bar{t}$		$\bar{s}$	
	Calculated from (3.10)	Numerical (Table 2)	Calculated from (3.12)	Numerical (Table 2)
1. $d = 11.17$, $b_o = 1.5$	1.65	1.66	+.039	+.038
2. $d = 11.17$, $b_o = 1.17$	1.70	1.70	+.012	+.014
3. $d = 11.17$, $b_o = 1.08$	1.72	1.71	+.002	+.004
4. $d = 11.17$, $b_o = .9$	1.77	1.76	-.030	-.027
5. $d = \infty$, $b_o = 2.0$	1.61	1.61	-.026	-.025
6. $d = \infty$, $b_o = 1.5$	1.65	1.65	-.044	-.043
7. $d = \infty$, $b_o = 1.2$	1.70	1.70	-.067	-.065

Appendix II. The Velocity Potential for a Pulsating Sphere Moving Perpendicularly to a Wall.

1. Statement of the problem.

An ideal incompressible fluid is bounded by a plane infinite rigid wall,* and has a pulsating and moving sphere immersed in it. It is required to find the velocity potential describing the (irrotational) flow, and to obtain the kinetic energy of the liquid. The case of a moving sphere is classical and can be found in the standard books on Hydrodynamics. The pulsating sphere, however, does not seem to be generally known and has certain features of interest. The treatment here follows [5].

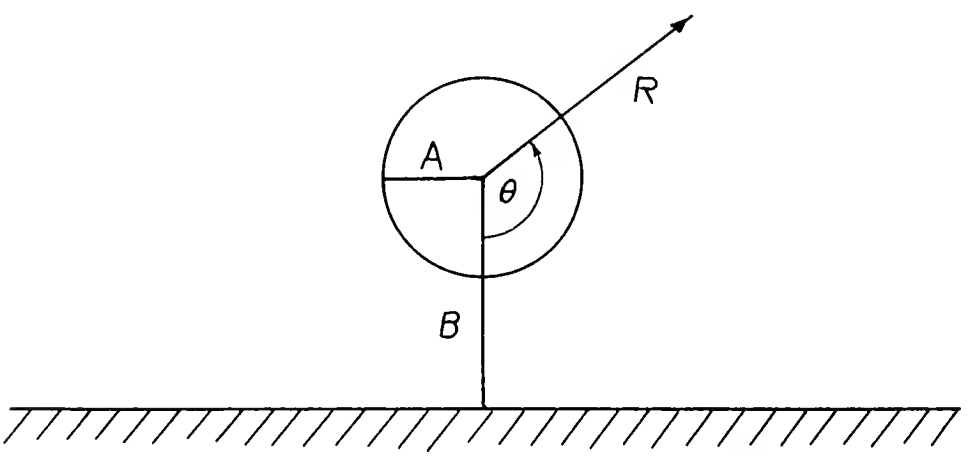

Let A be the radius of the sphere at any time T, and B the distance of its center from the rigid wall. The velocity potential Φ describing the flow of the liquid satisfies the potential equation

$$\triangle\Phi = \Phi_{xx} + \Phi_{yy} + \Phi_{zz} = 0$$

---

* The method used here can also be applied to a spherical wall.

and has the following boundary conditions:

$$(1)\qquad \begin{cases} -\dfrac{\partial \Phi}{\partial n} = A' - B' \cos\theta & \text{on the sphere} \\ -\dfrac{\partial \Phi}{\partial n} = 0 & \text{on the plane,} \end{cases}$$

where n is the normal direction pointing into the liquid and the "prime" denotes a time derivative.

The construction of Φ can be decomposed into two simpler problems by setting

$$(2)\qquad \Phi = A' \Phi_0 - B' \Phi_1$$

where Φ_0, Φ_1 are potential functions satisfying the following boundary conditions:

$$(3)\quad -\frac{\partial \Phi_0}{\partial n} = 1 \quad \text{on the sphere,} \quad -\frac{\partial \Phi_0}{\partial n} = 0 \quad \text{on the plane}$$

$$(4)\quad -\frac{\partial \Phi_1}{\partial n} = \cos\theta \quad \text{on the sphere,} \quad -\frac{\partial \Phi_1}{\partial n} = 0 \quad \text{on the plane.}$$

Physically, Φ_0 represents the potential function for a sphere of fixed center and radius expanding with unit velocity, while Φ_1 is the function associated with a rigid sphere moving away from the wall at unit velocity. The functions Φ_0, Φ_1 will be constructed by means of the method of images.

2. Some theorems on images.

The theorems that follow supplement well known theorems on images. See Milne-Thomson, Theoretical Hydrodynamics, Chapter 15.

We wish to find a potential function Φ, defined outside a given sphere, with a given distribution of sources outside the sphere and vanishing normal derivative, $\frac{\partial \Phi}{\partial n} = 0$, on the boundary. A standard method for constructing Φ is to place a suitable arrangement of sources inside the sphere, called the image of the original distribution.

The image of a point source and a radial dipole are well known, and will be found in Milne-Thomson, pp. 420,421. Here we consider the image of a line source.

Theorem 1. Consider a sphere with center 0 and radius a. The image of a uniform line source of strength μ per unit length stretching from Q_1 to Q_2 is the following: a uniform line source of strength $\mu \frac{\overline{OQ_2}}{a}$ per unit length, stretching between the points Q_1', Q_2' inverse to Q_1, Q_2, and a uniform line sink of strength $\mu \frac{\overline{Q_1 Q_2}}{a}$ per unit length extending from 0 to Q_1'.

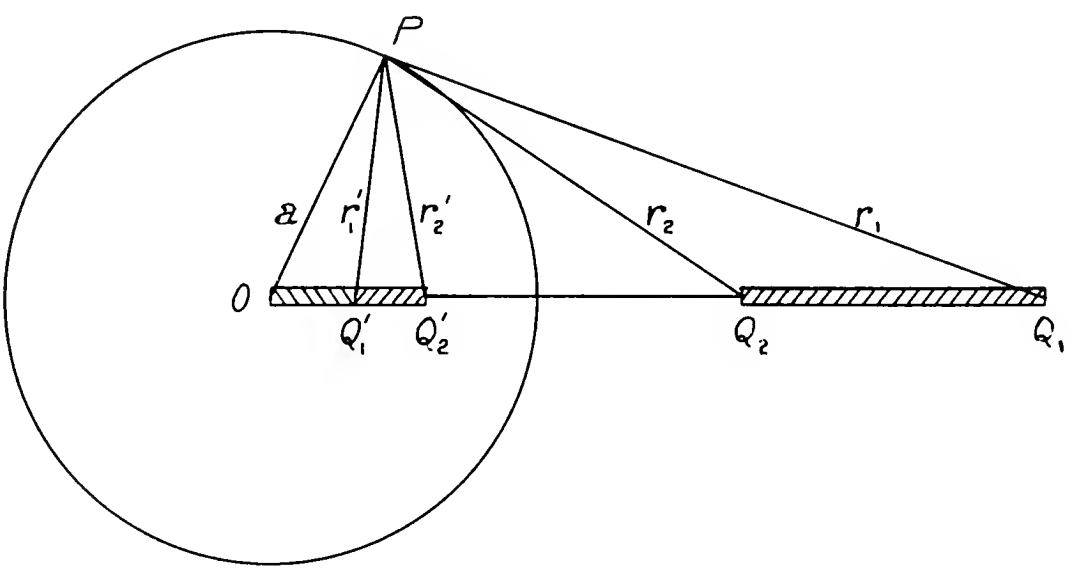

Proof. If P is any point, the Stokes stream function Ψ (see Milne-Thomson, Chapter 15, esp. pp. 420, 421) is

$$\Psi = -\mu \frac{\overline{Q_1Q_2}}{a}(r-r_1') + \mu \frac{\overline{OQ_2}}{a}(r_1'-r_2') + \mu(r_2-r_1) .$$

If P is on the sphere, we have $r_1' = \frac{a}{\overline{OQ_1}} r_1$, $r_2' = \frac{a}{\overline{OQ_2}} r_2$ (a property of inverse points, due to the similarity of triangles OPQ_1', OQ_1P), and consequently $\Psi = -\mu \frac{\overline{Q_1Q_2}}{a} = \text{const.}$ Therefore $\frac{\partial \Phi}{\partial n} = 0$ on the sphere.

Combining this result with the known image of a point source (Milne-Thomson, pp. 420,421), we obtain the following:

Theorem 2. The image of a point source of strength m situated at the point Q_2, together with a uniform line sink of strength μ per unit length extending from Q_1 to Q_2, where $m = \mu\overline{Q_1Q_2}$ (so that the total strength is zero), is the following: a point source of strength $m \frac{a}{\overline{OQ_2}}$ at the point Q_2' and a uniform line sink of strength $\mu \frac{\overline{OQ_1}}{a}$ per unit length extending between Q_1', Q_2'.

3. The construction of Φ_o.

The function Φ_o is required to satisfy the boundary conditions (3). If the plane were not present, Φ_o would be $\frac{A^2}{R}$, which represents a source of strength A^2 placed at O. The presence of the plane, however, causes the boundary condition (3) on the plane to be violated. To satisfy it, introduce the image of the source relative to the plane, which is a source of equal strength at the reflected point Q_1. But the boundary condition on the sphere is now violated, and to

remedy it, introduce the image of the point source at Q_1 relative to the sphere. This image is a point source of strength $A\frac{2A}{\overline{OQ}_1}$ at the inverse point Q_1' and a uniform line sink of strength $A^2\frac{1}{A}$ per unit length extending from 0 to Q_1'; this process continues and requires the use of theorem 2 for the images relative to the sphere. The successive images fit very neatly together, as indicated in the diagram.

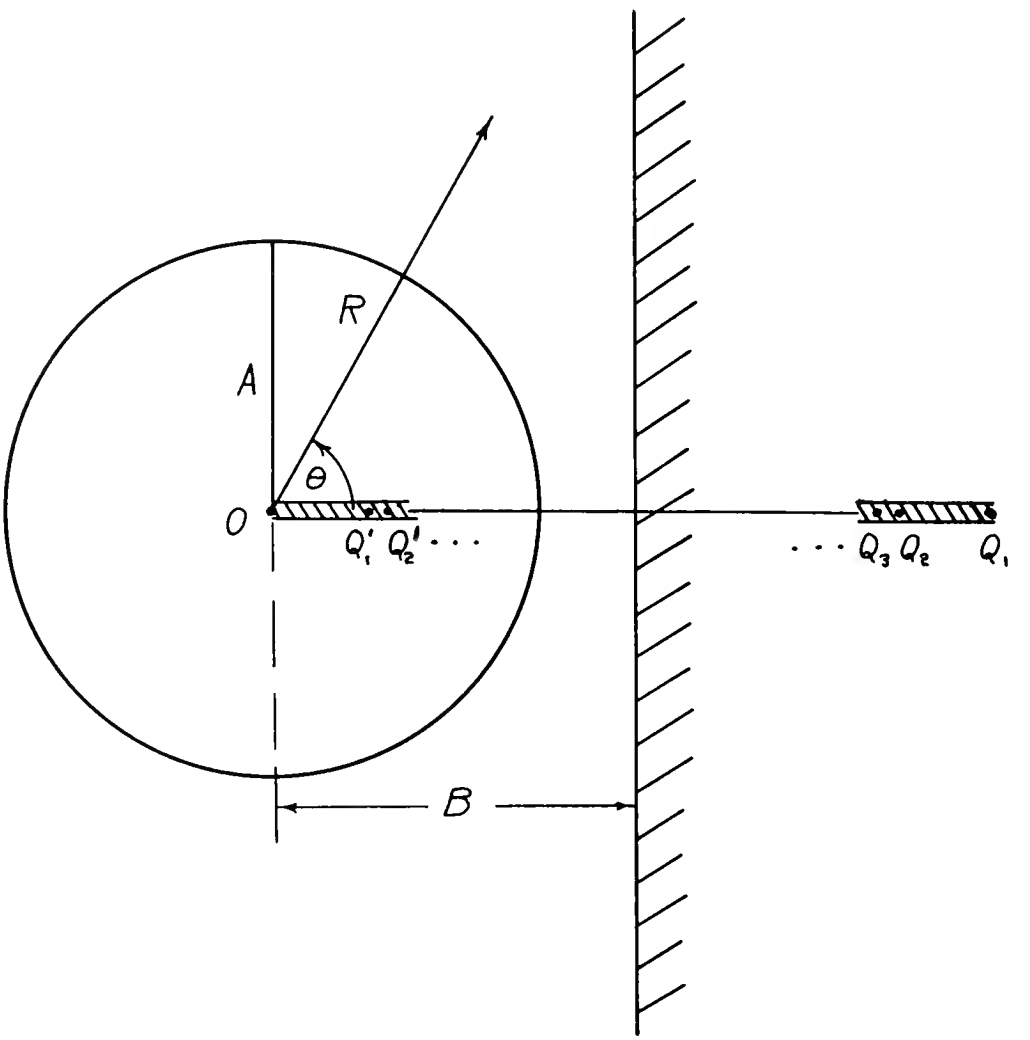

The successive reflections are described in the following table:

Strength of point source	Situation of point source	Strength per unit length of uniform line sink	Situation of uniform line sink
A^2	0		
A^2	Q_1		
$A^2\frac{A}{\overline{OQ_1}}$	Q_1'	A	OQ_1'
$A^2\frac{A}{\overline{OQ_1}}$	Q_2	A	Q_1Q_2
$A^2\frac{A}{\overline{OQ_1}}\frac{A}{\overline{OQ_2}}$	Q_2'	$A\frac{\overline{OQ_1}}{A}$	$Q_1'Q_2'$

etc.

Set

$$d_n = \frac{A}{\overline{OQ_n}} \tag{5}$$

and

$$D_n = d_1 \cdot d_2 \cdot \cdots \cdot d_n \quad . \tag{6}$$

By the inversion, d_n is also equal to $\frac{\overline{OQ_n'}}{A}$. The general expressions for the strengths of the sources are:

(7) { A point source of strength AD_n at Q_n' and Q_{n+1}; a uniform line sink of strength $\frac{A}{D_n}$ per unit length along $Q_n'Q_{n+1}'$ and $Q_{n+1}Q_{n+2}$.

Introduce the quantity

$$\alpha = \frac{A}{2B} \quad . \tag{8}$$

The quantities d_n can be expressed in terms of α. We have

$$d_{n+1} = \frac{A}{\overline{OQ}_{n+1}} = \frac{A}{2B - \overline{OQ}_n'} = \frac{1}{\frac{2B}{A} - d_n} \quad .$$

Thus

$$d_1 = \alpha, \ldots, \; d_{n+1} = \frac{1}{\frac{1}{\alpha} - d_n} \; , \ldots \; , \tag{9}$$

so that the d's are convergents to a continued fraction.

The quantities D_n can be obtained as functions of α from the definition (6). They can also be obtained by solving a second order linear difference equation with constant coefficients for the quantity $\frac{1}{D_n}$, obtained from the recursion formula (9).

It is convenient to expand Φ_o in the neighborhood of the surface of the sphere in terms of spherical harmonics. The expansion of a unit point source lying outside the sphere at a distance X from the center is

$$\frac{1}{X} + \frac{R}{X^2} P_1(\cos\theta) + \frac{R^2}{X^3} P_2(\cos\theta) + \ldots \; , \tag{10}$$

while a point source lying inside the sphere has an expansion

$$\frac{1}{R} + \frac{X}{R^2} P_1(\cos\theta) + \frac{X^2}{R^3} P_2(\cos\theta) + \ldots \; , \tag{11}$$

where $\{P_n(\cos\theta)\}$ are the Legendre polynomials of $\cos\theta$. (See diagram on page 41). Integration with respect to X yields the expansion of a uniform line source. The expansion of Φ_o is then easily obtained by using the distribution of sources and sinks given in (7).

For the present purpose it suffices to know merely the value of $\frac{1}{4\pi A^2}\int_K \Phi_o dS$, the mean value of Φ_o over the surface K of the sphere. The integral of a unit point source over the surface of the sphere is, by (10) and (11),

$$(12) \qquad \frac{1}{X} \quad \text{or} \quad \frac{1}{A},$$

according as the source lies outside or inside the sphere. The first of these is to be expected from the mean value theorem for potential functions, while the second is a constant, independent of the position of the sources inside the sphere.

The value of $\frac{1}{4\pi A^2}\int_K \Phi_o dS$ can now be obtained by using the distribution of sources and line sinks (7). The contribution of the distribution <u>inside</u> the sphere reduces to $A^2\frac{1}{A}$ due to the source of strength A^2 at the center. This follows from the second result in (12) and the fact that the successive images, each consisting of a source and a line sink, have a total strength zero. The contribution due to the source A^2D_n at Q_{n+1} and the line sink of strength $\frac{A}{D_{n-1}}$ per unit length along Q_nQ_{n+1} (see equation (7)) is

$$A^2D_n\frac{1}{\overline{OQ}_{n+1}} - \frac{A}{D_{n-1}}\log\frac{\overline{OQ}_n}{\overline{OQ}_{n+1}},$$

or

$$A\,D_{n+1} - \frac{A}{D_{n-1}}\log\frac{d_{n+1}}{d_n},$$

by (5) and (6). Thus we obtain the final result

$$(13)\qquad \int_K \Phi_o dS = 4\pi A^3 \left[1 + D_1 + \sum_{n=1}^{\infty} \left(D_{n+1} - \frac{1}{D_{n-1}} \log \frac{d_{n+1}}{d_n} \right) \right].$$

The term D_1 is due to the point source A^2 at Q_1.

4. The construction of Φ_1.

The function Φ_1 is required to satisfy the boundary conditions (4). If the plane were not present, Φ_1 would be the velocity potential due to a dipole of strength $\frac{A^3}{2}$ placed at 0, namely, $\frac{A^3}{2} \frac{\cos\theta}{R^2}$. The boundary condition on the plane, however, is violated and to satisfy it, introduce the image radial dipole of strength $-\frac{A^3}{2}$ situated at the reflected point Q_1 (see the diagram on page 45). To remedy this boundary condition on the sphere, which has now been violated, introduce the image of this radial dipole relative to the sphere. This image is another radial dipole of strength $\frac{A^3}{2} \frac{A^3}{\overline{OQ_1}^3}$ at the inverse point Q_1'. (See Milne-Thomson, p. 421). Etc.

The successive reflections are described in the following table:

Strength of Dipole	Situation of Dipole
$\frac{A^3}{2}$	0
$-\frac{A^3}{2}$	Q_1
$\frac{A^3}{2} \frac{A^3}{\overline{OQ_1}^3}$	Q_1'
$-\frac{A^3}{2} \frac{A^3}{\overline{OQ_1}^3}$	Q_2
$\frac{A^3}{2} \frac{A^3}{\overline{OQ_1}^3} \frac{A^3}{\overline{OQ_2}^3}$	Q_2'

etc.

The general expressions for the strengths of the dipoles are:

$$(14)\quad \begin{cases} \text{at } Q_n' \text{ , there is a radial dipole of strength } \frac{A^3}{2} D_n^3 \text{ ;} \\ \text{at } Q_{n+1}, \text{ " " " " " " " } - \frac{A^3}{2} D_n^3 \text{ .} \end{cases}$$

The expansion of a unit radial dipole lying outside a sphere at a distance X from the center is

$$(15)\quad -\frac{1}{X^2} - \frac{2R}{X^3} P_1(\cos\theta) - \frac{3R^2}{X^4} P_2(\cos\theta) - \cdots\cdots ,$$

while a radial dipole inside the sphere has an expansion

$$(16)\quad \frac{1}{R^2} P_1(\cos\theta) + \frac{2X}{R^3} P_2(\cos\theta) + \cdots\cdots .$$

These are obtained from (10), (11) by differentiation with respect to X. See Milne-Thomson, pp. 442,443.

For the present purpose we are interested in the expansion of Φ_1 only up to terms involving $P_1(\cos\theta)$.

Using (14), (15), (16), we obtain

$$(17)\quad \Phi_1 = \frac{A^3}{2} \sum_{n=0}^{\infty} \frac{D_n^3}{\overline{OQ}_{n+1}^2} + A^3 \sum_{n=0}^{\infty} \frac{D_n^3}{\overline{OQ}_{n+1}^3} R\, P_1(\cos\theta)$$

$$+ \frac{A^3}{2} \sum_{n=0}^{\infty} D_n^3 \frac{P_1(\cos\theta)}{R^2} + \text{terms in higher Legendre polynomials.}$$

It is convenient to evaluate $\int_K \Phi_1 dS$ and $\int_K \Phi_1 \cos\theta\, dS$. Using the orthogonality property of Legendre polynomials,

and (17), (5), (6), we have

$$(18) \qquad \int_K \Phi_1 dS = 2\pi A^3 \sum_{n=0}^{\infty} D_n^3 \, d_{n+1}^2$$

$$(19) \qquad \int_K \Phi_1 \cos\theta dS = \frac{2}{3}\pi A^3 (1 + 3\sum_{n=1}^{\infty} D_n^3) \quad .$$

5. The kinetic energy of the water.

The kinetic energy $\mathcal{T}$ of the water is

$$\mathcal{T} = \frac{1}{2}\rho \int (\text{grad } \Phi)^2 dV = -\frac{1}{2}\rho \int \Phi \frac{\partial \Phi}{\partial n} dS$$

by Green's theorem. By (2), and the Green's theorem

$$\int \Phi_o \frac{\partial \Phi_1}{\partial n} dS = \int \Phi_1 \frac{\partial \Phi_o}{\partial n} dS,$$

$$\mathcal{T} = -\frac{1}{2}\rho \left[\dot{A}^2 \int \Phi_o \frac{\partial \Phi_o}{\partial n} dS - 2\dot{A}\dot{B} \int \Phi_1 \frac{\partial \Phi_o}{\partial n} dS + \dot{B}^2 \int \Phi_1 \frac{\partial \Phi_1}{\partial n} dS \right] \quad .$$

The boundary conditions (3), (4) yield

$$(20) \quad \mathcal{T} = \frac{1}{2}\rho \left[\dot{A}^2 \int_K \Phi_o \, dS - 2\dot{A}\dot{B} \int_K \Phi_1 dS + \dot{B}^2 \int_K \Phi_1 \cos\theta dS \right] \quad .$$

The integrals appearing in (20) have been calculated in the preceding sections. By (13), (18), (19),

$$(21) \quad \mathcal{T} = 2\pi\rho A^3 \left[(1+f_o)\dot{A}^2 - 2f_1 \dot{A}\dot{B} + (\tfrac{1}{6}+f_2)\dot{B}^2 \right] ,$$

where the coefficients f_o, f_1, f_2 are the following functions of the quantity $\alpha = \frac{A}{2B}$:

$$(22)\quad \begin{cases} f_o = D_1 + \sum_{n=1}^{\infty} \left[D_{n+1} - \frac{1}{D_{n-1}} \log \frac{d_{n+1}}{d_n} \right] \\ f_1 = \frac{1}{2} \sum_{n=o}^{\infty} D_n^3 \, d_{n+1}^2 \\ f_2 = \frac{1}{2} \sum_{n=1}^{\infty} D_n^3 \quad . \end{cases}$$

The expressions for d_n, D_n as functions of α are given in (9) and (6).

The series for f_o, f_1, f_2 converge for $\alpha \leqq 1/2$ (which means $A \leqq B$). They are tabulated in table 4 below. Expansions in powers of α begin as follows:

$$f_o = \alpha + \frac{1}{2}\alpha^4 + \cdots$$

$$f_1 = \frac{1}{2}\alpha^2 + \frac{1}{2}\alpha^5 + \cdots$$

$$f_2 = \frac{1}{2}\alpha^3 + \frac{1}{2}\alpha^6 + \cdots$$

The expansions for $\sqrt{1 + f_o}$, $\frac{df_o/d\alpha}{\sqrt{1 + f_o}}$ required in part III, begin as follows:

$$(24)\quad \begin{cases} \sqrt{1 + f_o} = 1 + \frac{1}{2}\alpha \\ \frac{df_o/d\alpha}{\sqrt{1 + f_o}} = 1 - \frac{1}{2}\alpha + \quad . \end{cases}$$

α	f_o	f_1	f_2	$\frac{df_o}{d\alpha}$	$\frac{df_1}{d\alpha}$	$\frac{df_2}{d\alpha}$
0	0	0	0	1.00	0	0
.02	.020	.000	.000	1.00	.02	.00
04	040	001	000	1.00	04	00
06	060	002	000	1.00	06	01
08	080	003	000	1.00	08	01
.10	.100	.005	.001	1.00	.10	.02
12	120	007	001	1.00	12	02
14	140	010	001	1.01	14	03
16	160	013	002	1.01	16	04
18	181	016	003	1.01	18	05
.20	.201	.020	.004	1.02	.20	.06
22	221	024	005	1.03	23	07
24	242	029	007	1.03	25	09
26	263	035	009	1.04	28	11
28	283	040	011	1.05	30	13
.30	.305	.047	.014	1.08	.33	.15
32	326	053	017	1.09	36	17
34	348	061	021	1.11	39	20
36	371	070	025	1.15	43	23
38	394	078	030	1.18	48	27
.40	.418	.088	.036	1.23	.53	.32
41	430	094	039	1.26	57	35
42	443	100	043	1.29	60	38
43	456	106	047	1.34	65	42
44	470	112	051	1.40	69	46
.45	.484	.120	.056	1.45	.76	.52
46	499	128	062	1.54	84	60
47	515	136	068	1.64	95	70
48	532	147	076	1.81	1.12	86
49	551	159	085	2.26	1.55	1.27
.50	.577	.178	.101	∞	∞	∞

Table 4.

A comparison with the complete table shows that $1 + \frac{\alpha}{2}$ is a very close approximation to $\sqrt{1 + f_o}$ for all $\alpha \leq \frac{1}{2}$, and differs from it by less than 1 percent. On the other hand, $1 - \frac{\alpha}{2}$ is not too good an approximation to $\frac{df_o/d\alpha}{\sqrt{1 + f_o}}$. Further terms in the expansion of $\frac{df_o/d\alpha}{\sqrt{1 + f_o}}$ are not necessary since they produce only small deviations from the formulas (3.12) and (3.11).

6. Approximate theory for a sphere pulsating between a rigid wall and a free surface.

Consider a pulsating bubble at a distance b from a rigid wall and a distance c from a free surface.* For convenience, the free surface will appear vertical in the diagram.

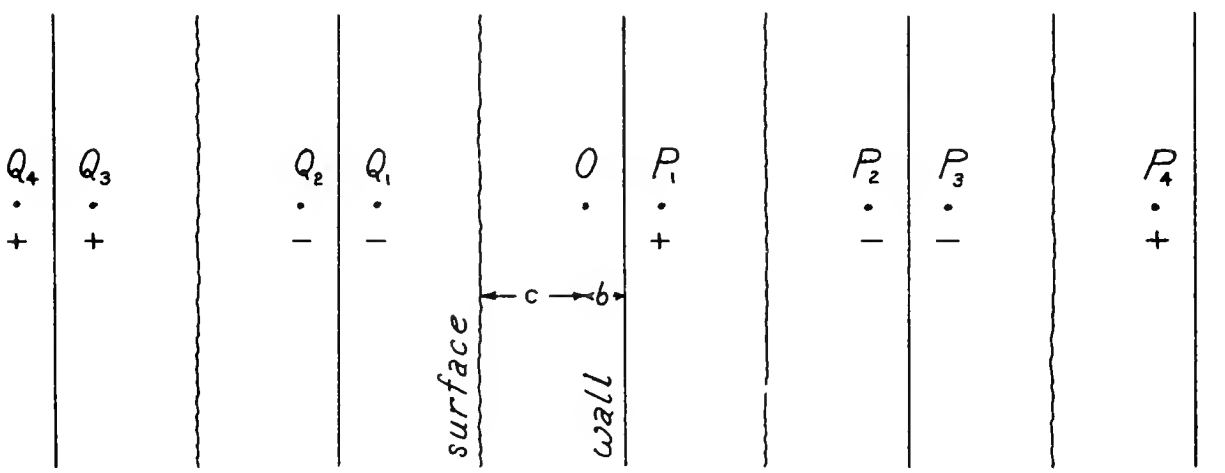

If O is the original position of the center of the sphere, the successive images with respect to the rigid wall and free surface will be at P_1, Q_1; P_2, Q_2; P_3, Q_3; etc. Their distances from O will be given by the following

---

* See [6].

formulas:

$$\overline{OP}_n = 2m(b+c) \qquad \text{if} \quad n = 2m$$

$$= 2m(b+c) + 2b \qquad \text{if} \quad n = 2m + 1$$

$$\overline{OQ}_n = 2m(b+c) \qquad \text{if} \quad n = 2m$$

$$= 2m(b+c) + 2c \qquad \text{if} \quad n = 2m + 1$$

The signs of the images are given in the diagram.

Images with respect to the sphere will be neglected.

The first term in the expansion of f_o in powers of a can be obtained by finding the potential at O of the infinite series of images P_1, Q_1, P_2, Q_2, etc. Some simple algebraic transformations lead to the formula

$$f_o = \frac{a}{b+c}(2xf(x) - \log 2)$$

where $x = \frac{c - b}{c + b}$ and

$$f(x) = \frac{1}{1-x^2} - \frac{1}{9-x^2} + \frac{1}{25-x^2} \cdots$$

It is to be noted that

$$\frac{\partial f_o}{\partial b} = - \frac{4a}{(b+c)^2} [f(x) + xf'(x)]$$

To facilitate comparison with previous results,

f_o and $\frac{\partial f_o}{\partial b}$ can be written as follows:

$$f_o = \frac{a}{2b}(1-x)(2xf(x) - \log 2) = \frac{a}{2b}F(x)$$

$$\frac{\partial f_o}{\partial b} = -\frac{a}{2b^2}2(1-x)^2[f(x) + xf'(x)] = -\frac{a}{2b^2}G(x)$$

A short table for $F(x)$ and $G(x)$ is given on page 36.

Appendix III. Numerical Evaluation of Some Definite Integrals

In part III, the problem of evaluating the definite integrals in equations (3.7), (3.11) arose. These integrals have square root singularities at the limits of integration. In this appendix we shall develop a quadrature formula, which was used for this evaluation but does not seem to be as well-known as it should. It is based on Tchebycheff polynomials.

The nth Tchebycheff polynomial $T_n(x)$, $-1 \leqq x \leqq 1$, is defined by

$$T_n(x) = \cos(n \arccos x),$$

or in other terms, $T_n(x) = \cos n\theta$, where $x = \cos\theta$. The Tchebycheff polynomials are orthogonal with respect to the weight function $\frac{1}{\sqrt{1-x^2}}$, i. e.,

$$\int_{-1}^{1} \frac{T_n(x)\, T_m(x)}{\sqrt{1-x^2}}\, dx = 0 \qquad \text{if} \quad n \neq m.$$

This follows immediately when we make the transformation $x = \cos\theta$.

By virtue of the orthogonality property, the following theorem can be proved:

Theorem. Let $x_1, x_2, \ldots, x_n$ be the n zeros of $T_n(x)$ in the range $-1 \leqq x \leqq 1$. Let $f(x)$ be any polynomial of degree at most $2n-1$. Then

$$\frac{1}{\pi}\int_{-1}^{1} \frac{f(x)}{\sqrt{1-x^2}}\, dx = \frac{1}{n}\sum_{i=1}^{n} f(x_i).$$

The proof is similar to the proof of the Gauss quadrature formula. This theorem indicates an exact evaluation of the integral involving $2n$ parameters (a polynomial of degree $2n-1$) in terms of n specially selected points. It is exactly analogous to the more well known Gauss quadrature formula, but it is simpler in two ways: the zeros $x_1,\dots,x_n$ of $T_n(x)$ are easy to obtain, since they are merely the zeros of $\cos n\theta$ where $x = \cos\theta$; and the weight factors multiplying $f(x_i)$ are all equal to $1/n$.

If $f(x)$ is not exactly equal to a polynomial of degree $2n-1$ but can be approximated by one, we can write the approximate quadrature formula

$$\frac{1}{\pi}\int_{-1}^{1}\frac{f(x)}{\sqrt{1-x^2}}\,dx \sim \frac{1}{n}\sum_{i=1}^{n} f(x_i) \quad .$$

The accuracy of this approximate formula depends on the closeness with which $f(x)$ can be approximated by polynomials of degree $2n-1$.

The integrals in question in part III are of the form

$$\int_{a_o}^{a_1}\frac{a^v}{\sqrt{1 - a^3 - \frac{k}{a^{3/4}}}}\,da$$

where v is some exponent, and a_o, a_1 are the two zeros of the expression under the square root sign. This can be written as

$$\int_{a_o}^{a_1} a^v \cdot \frac{\sqrt{(a_1 - a)(a - a_o)}}{\sqrt{1 - a^3 - \frac{k}{a^{3/4}}}} \cdot \frac{da}{\sqrt{(a_1 - a)(a - a_o)}} \quad .$$

where the function $a^{v} \cdot \frac{\sqrt{(a_1 - a)(a - a_o)}}{\sqrt{1 - a^3 - \frac{k}{a^{3/4}}}}$ has no singularities and is rather smooth. The integral can now be evaluated by using the Tchebycheff quadrature formula (changing the range of integration by a linear transformation from a_o, a_1 to -1, 1). The integrals were evaluated in this way by using the 5 zeros of $T_5(x)$, with the results stated in part III. The accuracy depends on the closeness with which the remaining factor $a^{v} \cdot \frac{\sqrt{(a_1-a)(a-a_o)}}{\sqrt{1 - a^3 - \frac{k}{a^{3/4}}}}$ can be approximated by a 9th degree polynomial. It is fortunate that the integrand need be computed only for 5 intermediate points. (Also, the values obtained by using the three zeros of $T_3(x)$ agree within 1 percent with the values quoted.)

It is of interest to see how the momentum $\bar{s}$ depends on the parameter k. If the explosion takes place near the surface, say for a model experiment, the value of k would be approximately .16. For k = .16, the computations yield

$$\bar{s} = -\frac{1}{b_o^2}\left(.127 - \frac{.022}{b_o}\right) + \frac{1}{d-b_o}\left(.760 + \frac{.165}{b_o}\right)$$

in place of (3.12). All the constants have increased, but the alternate additions and substractions tend to cancel these increases. Thus, the new equation for the stabilized position, where $\bar{s} = 0$, is

$$d = 6b_o^2 + 3.32b_o + .4$$

which is practically identical with (3.13). The total period for this case turns out to be

$$\bar{t} = 1.48\left(1 + \frac{.189}{b_o}\right)$$

which is practically identical with (3.10).

Finally, if the internal energy is neglected, i.e., if $k = 0$, the integrals become Beta functions and

$$\bar{s} = -\frac{1}{b_o^2}\left(.182 - \frac{.033}{b_o}\right) + \frac{1}{d-b_o}\left(.934 + \frac{.212}{b_o}\right)$$

$$\bar{t} = 1.49\left(1 + \frac{.203}{b_o}\right).$$

The stabilized position where $\bar{s} = 0$ is

$$d = 5.1b_o^2 + 3.1b_o + .4 .$$

These deviate somewhat from (3.12) and (3.13).

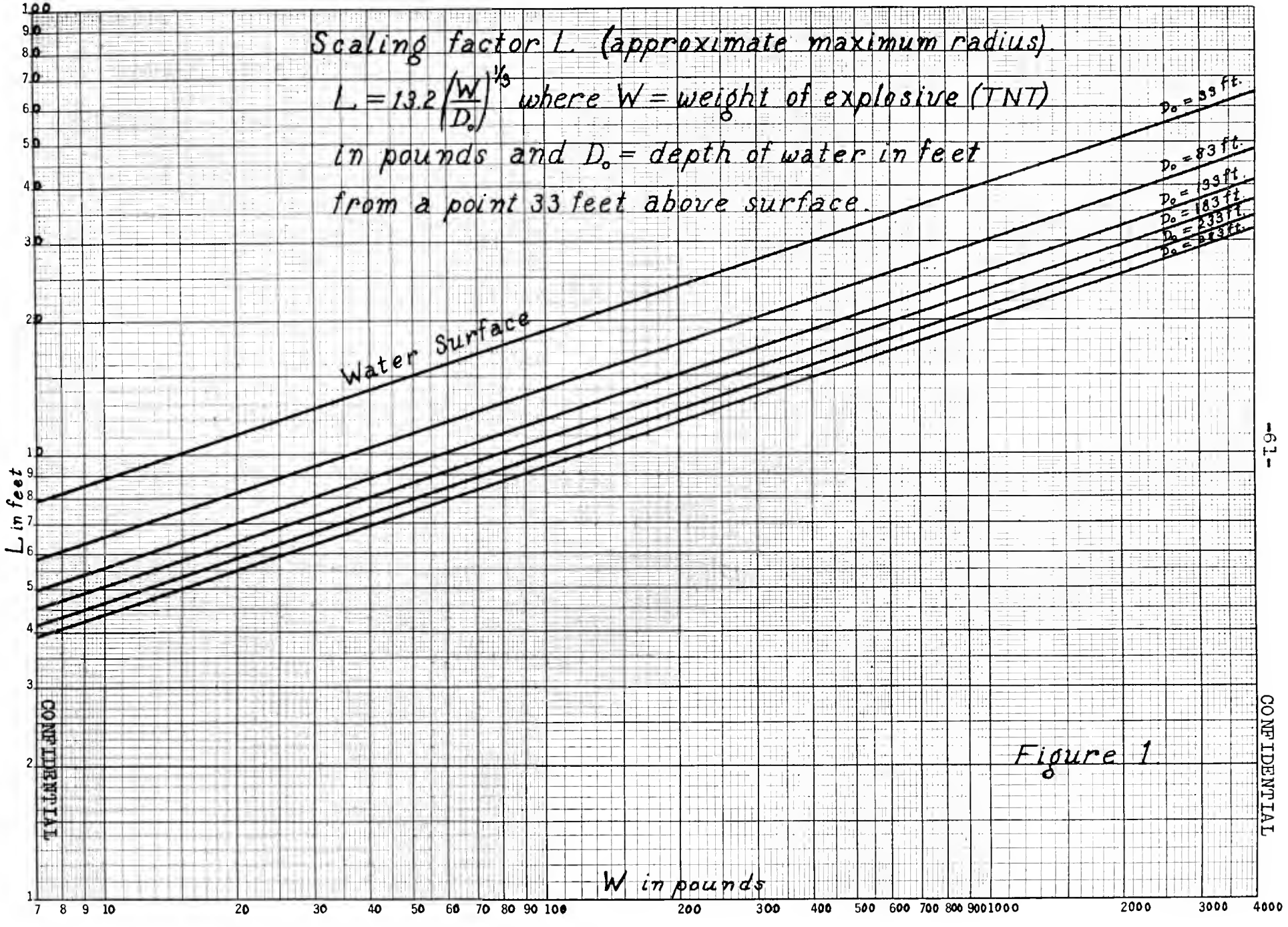

Figure 1

CONFIDENTIAL

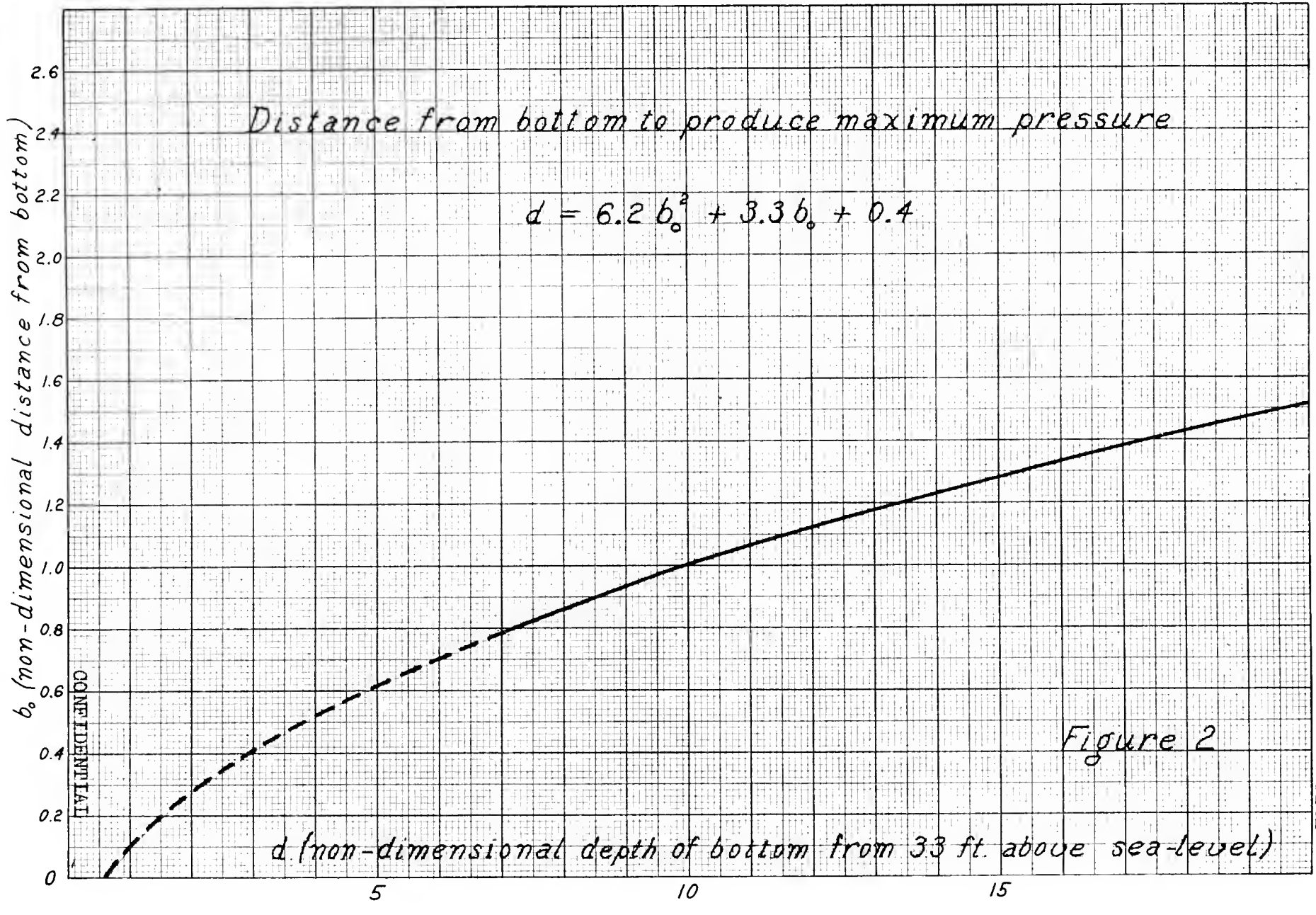

Figure 2

CONFIDENTIAL

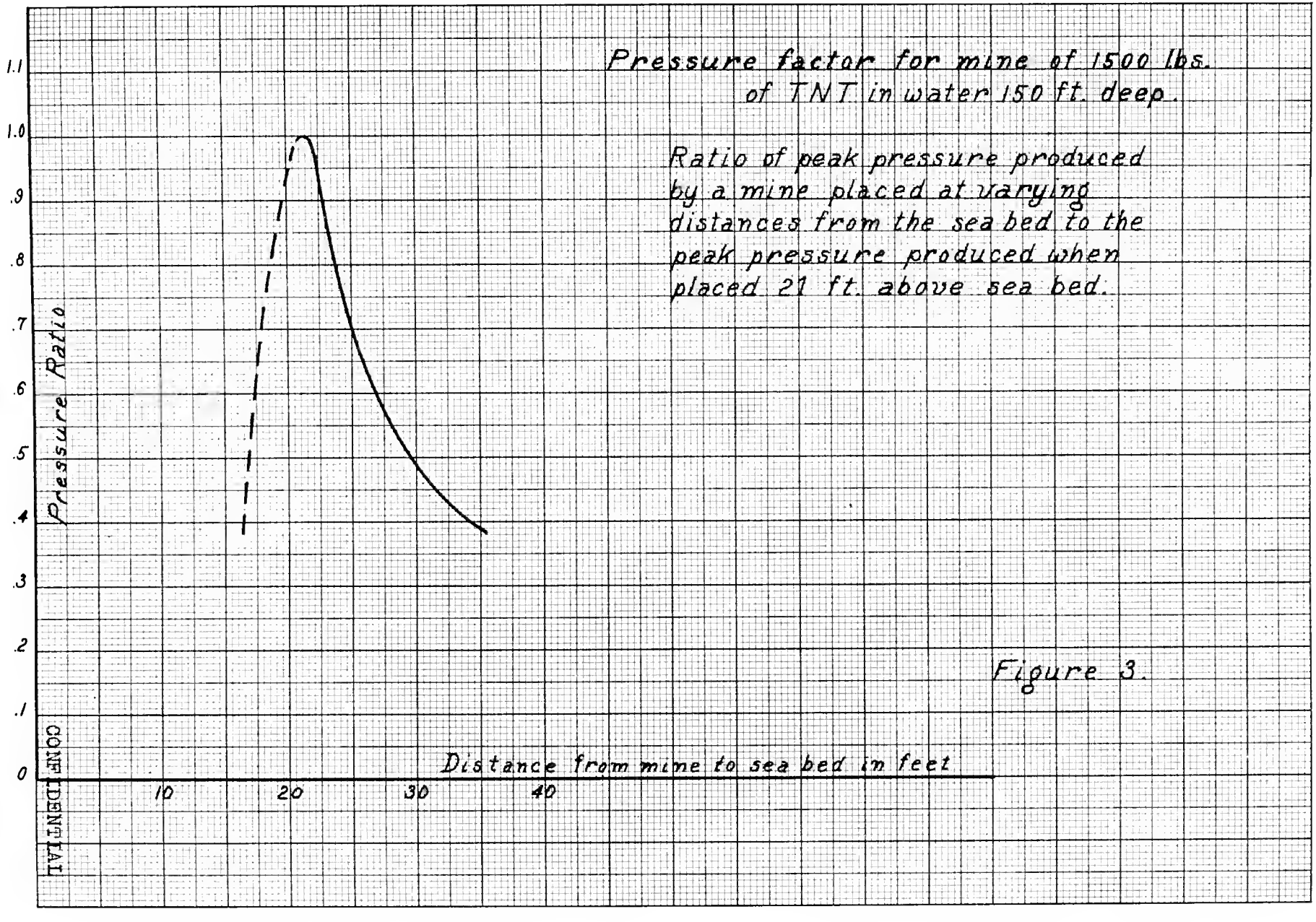

Figure 3.

CONFIDENTIAL

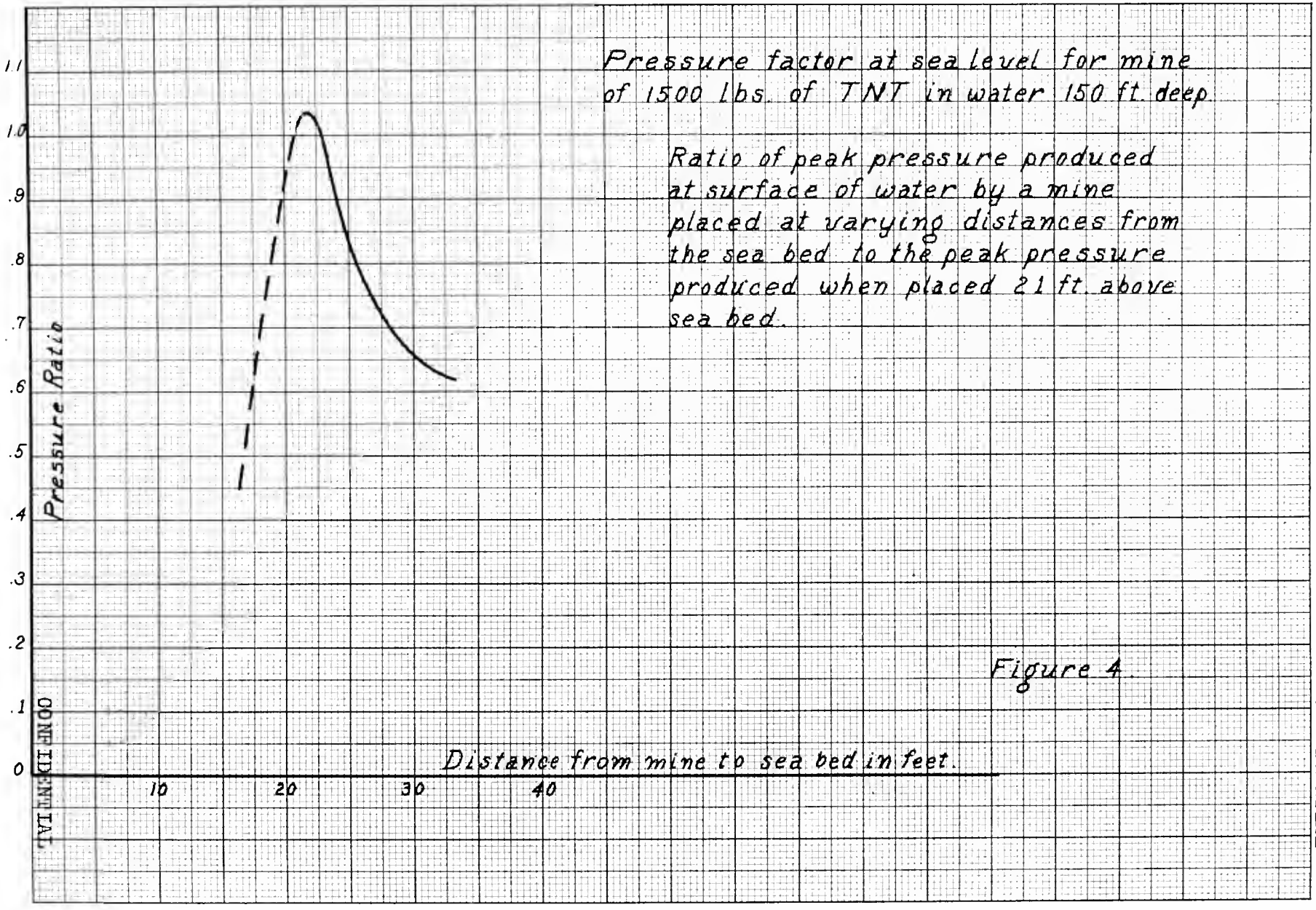

Figure 4.

Figure 5.

Dependence of internal energy ($\bar{u}$) on momentum ($\bar{s}$)

$\bar{u}$ (dimensionless internal energy of gas)

0.4 0.5 0.6 0.7 0.8 0.9 1.0

0 0.5 1.0 1.5 2.0 2.5 3.0 3.5 4.0

$\left(\frac{s}{s_{kr}}\right)$ where $\bar{s}$ = momentum (dimensionless).

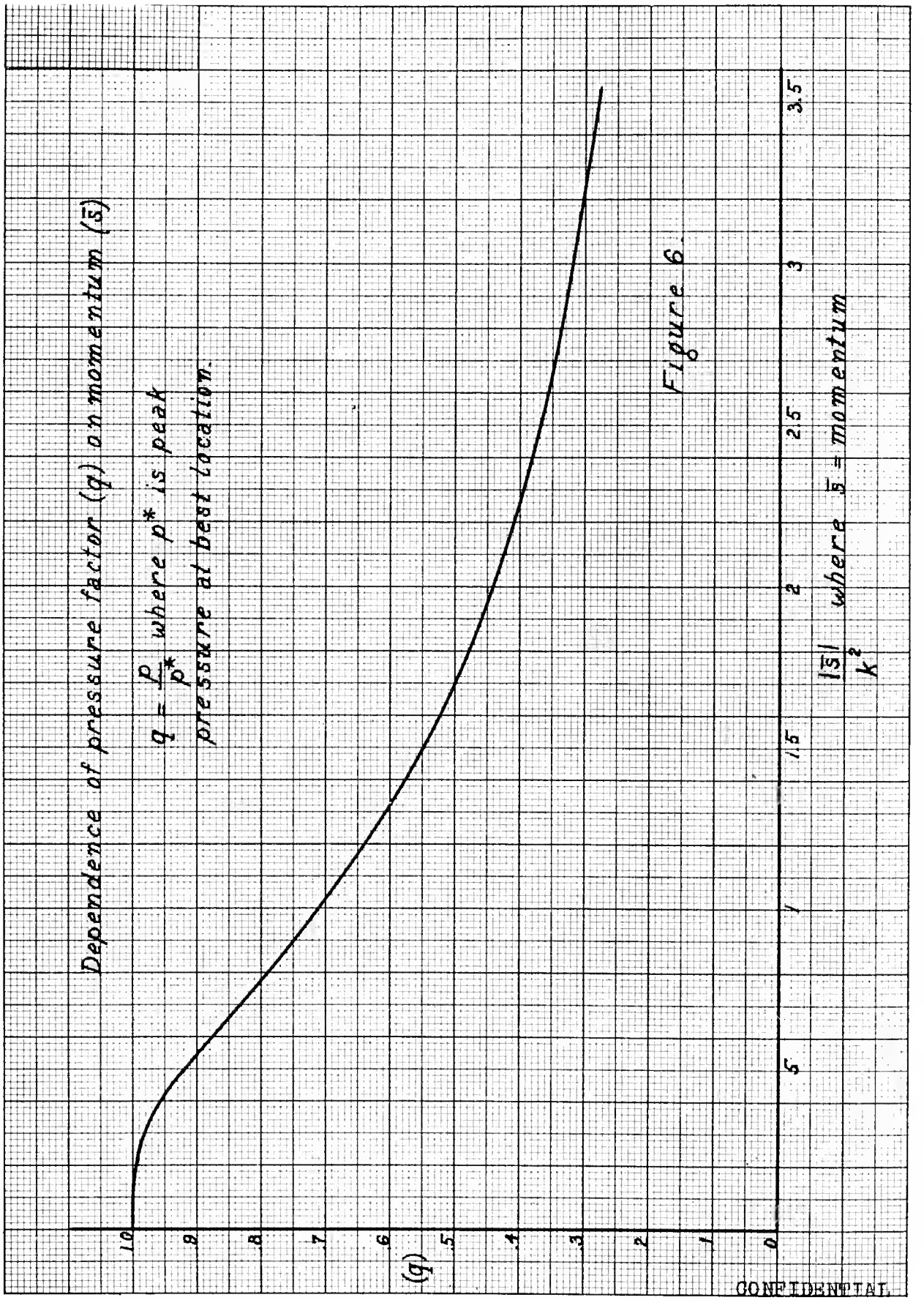
Dependence of pressure factor (q) on momentum (p̄)
q = p/p* where p* is peak pressure at best location.
(q)
1.0
.9
.8
.7
.6
.5
.4
.3
.2
.1
0
.5
1
1.5
2
2.5
3
3.5
|p̄| where p̄ = momentum
k²

Figure 6.

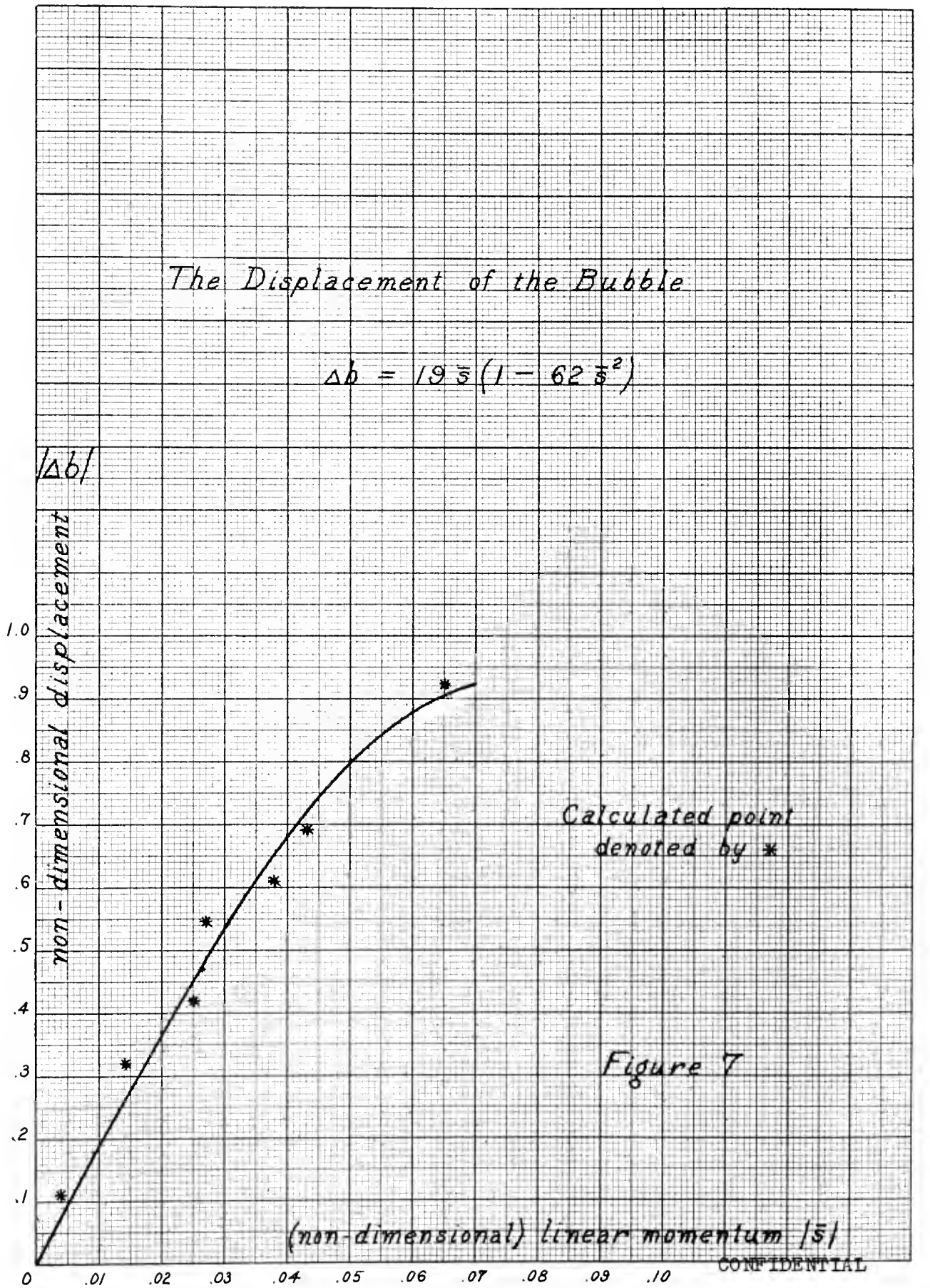
The Displacement of the Bubble
$\Delta b = 19\,\bar{s}\,(1 - 62\,\bar{s}^2)$
$|\Delta b|$
non-dimensional displacement
1.0
.9
.8
.7
.6
.5
.4
.3
.2
.1
0
.01
.02
.03
.04
.05
.06
.07
.08
.09
.10
Calculated point denoted by *
(non-dimensional) linear momentum $|\bar{s}|$

Figure 7

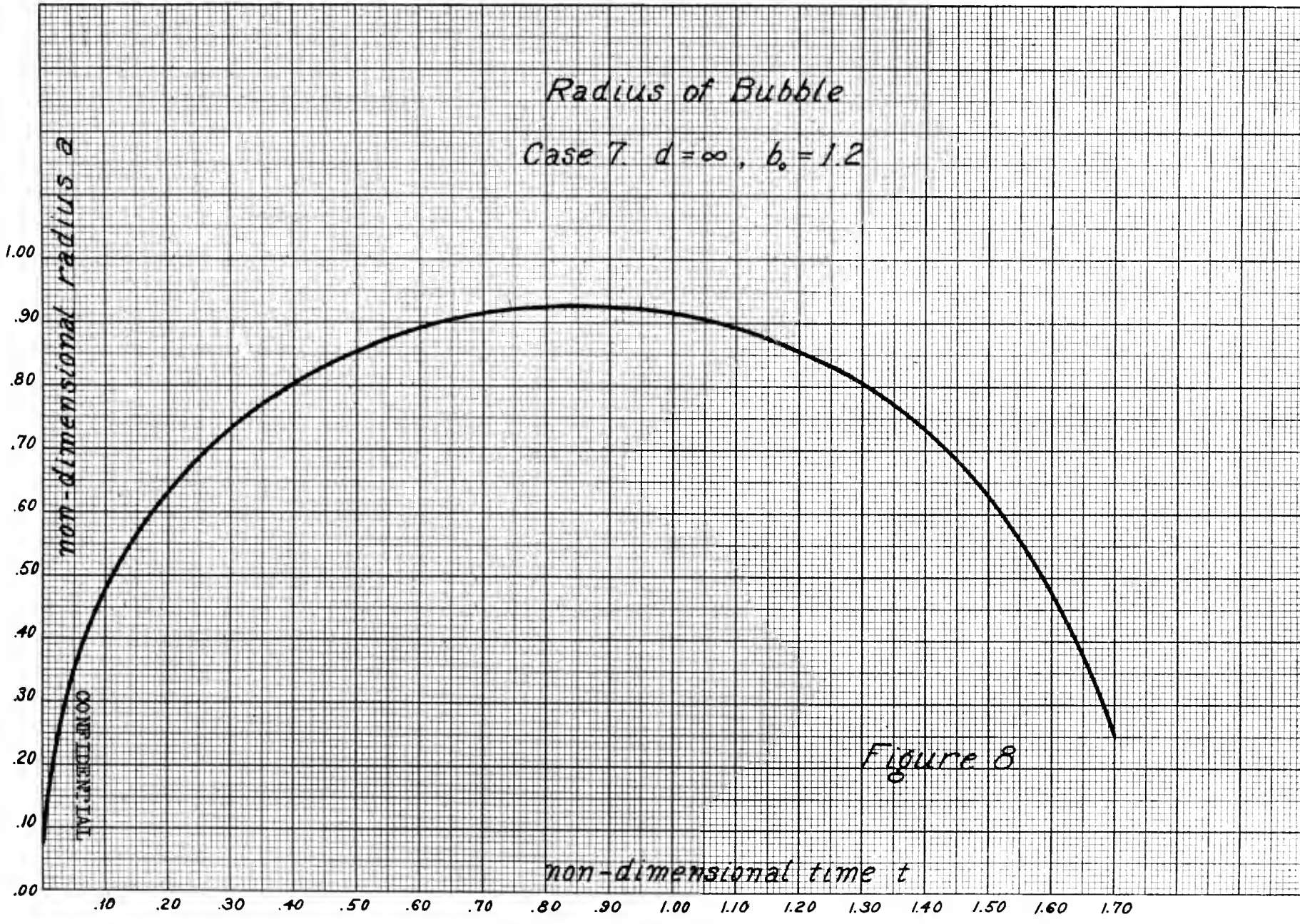

Figure 8

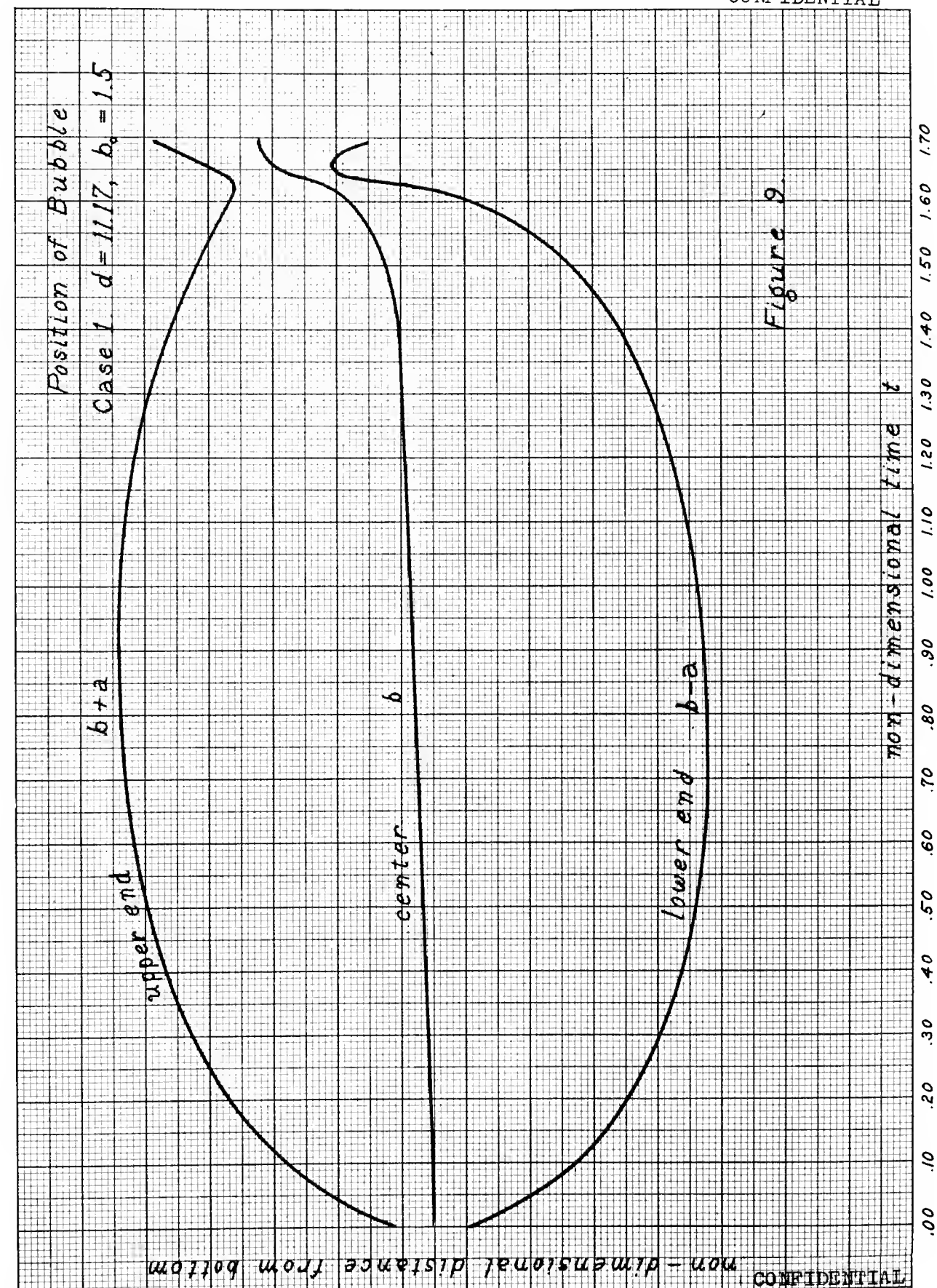
Position of Bubble
Case 1. d=11.17, b_o=1.5
b+a
upper end
b
center
lower end
b-a
non-dimensional distance from bottom
non-dimensional time t
2.80
2.60
2.40
2.20
2.00
1.80
1.60
1.40
1.20
1.00
.80
.60
.40
.20
.00
.00
.10
.20
.30
.40
.50
.60
.70
.80
.90
1.00
1.10
1.20
1.30
1.40
1.50
1.60
1.70

Figure 9

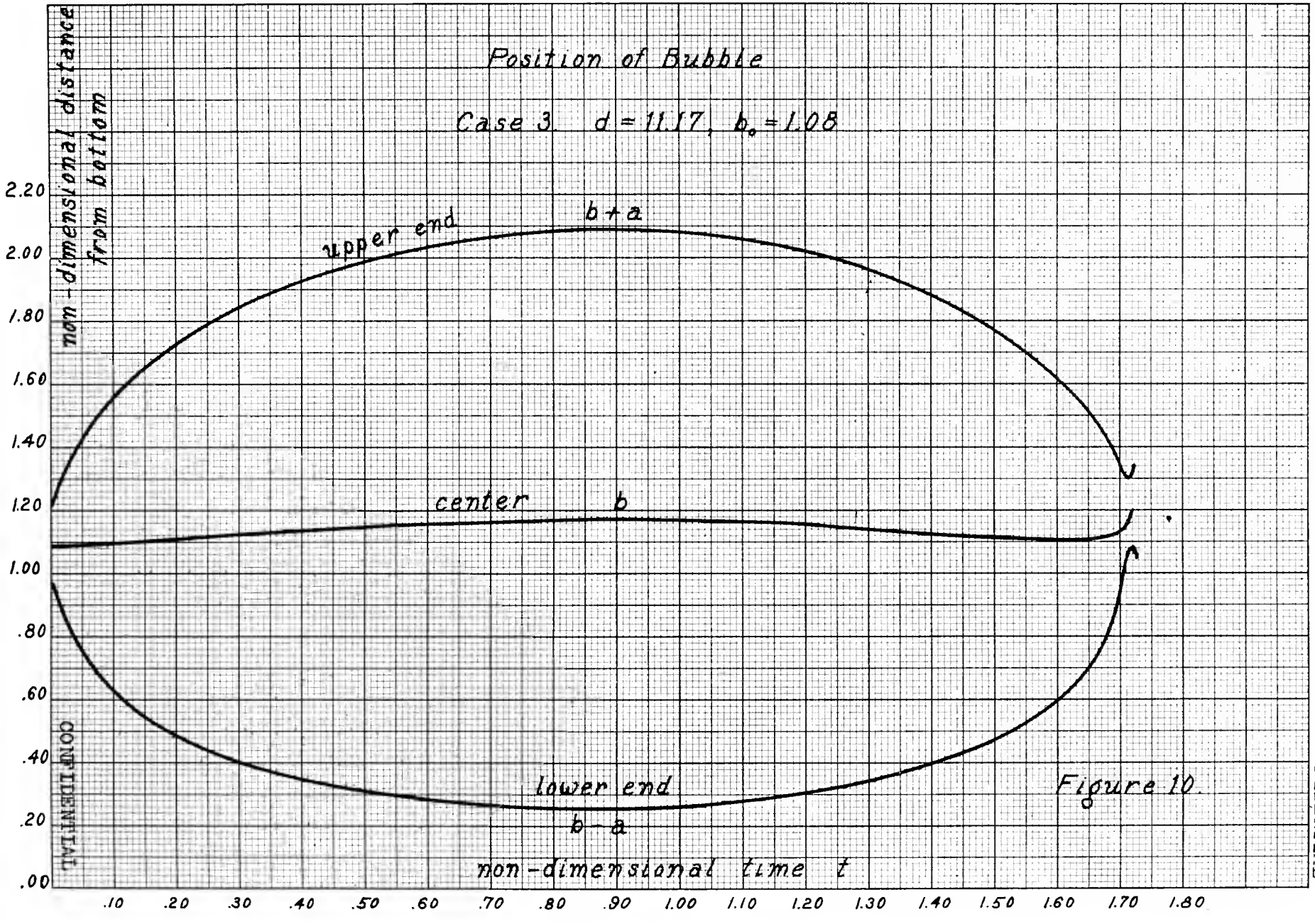

Figure 10.

CONFIDENTIAL

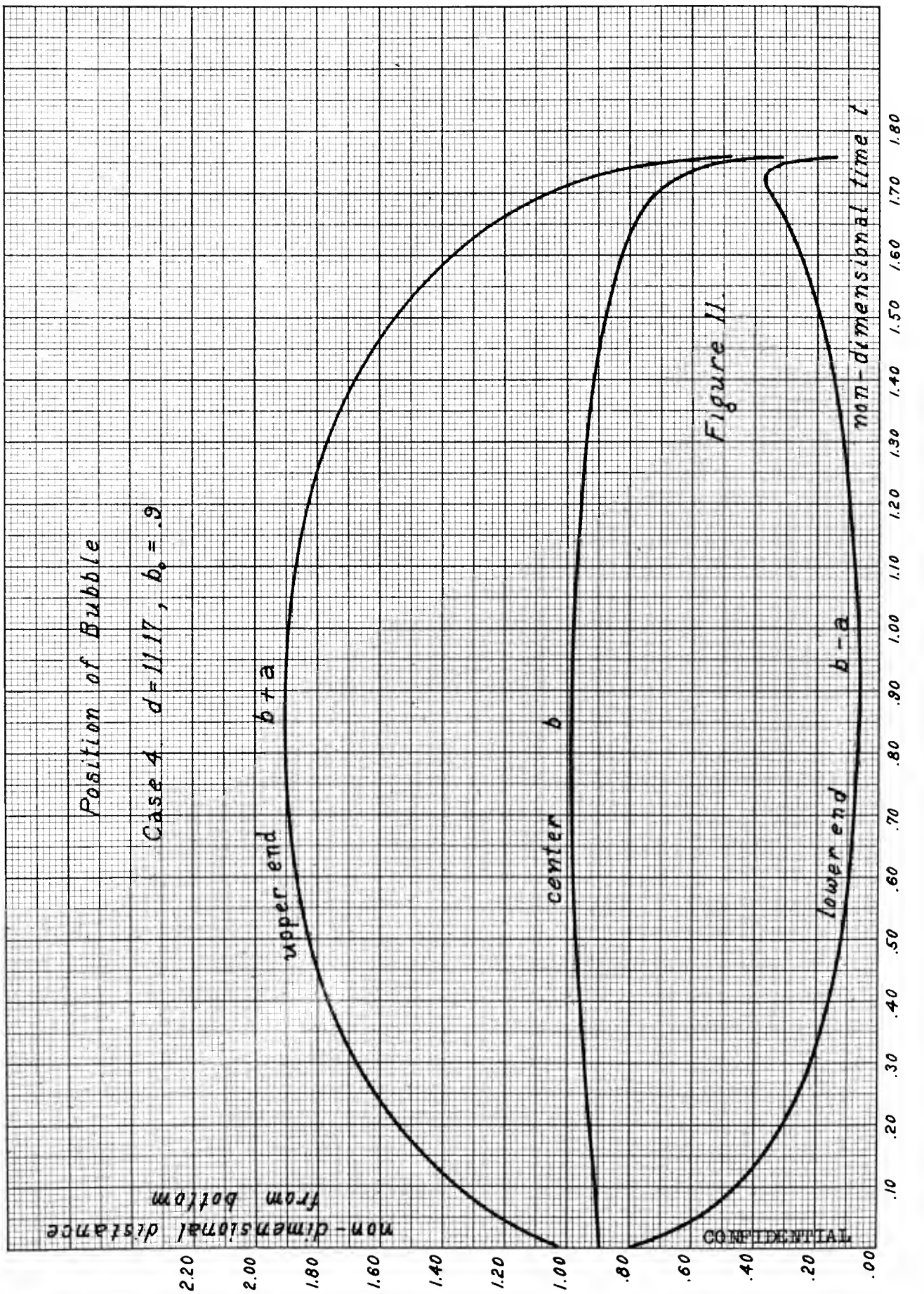
Position of Bubble
Case 4 d=11/17, b_o = .9
b + a
upper end
b
center
b - a
lower end
non-dimensional distance from bottom
2.20
2.00
1.80
1.60
1.40
1.20
1.00
.80
.60
.40
.20
.00
.10
.20
.30
.40
.50
.60
.70
.80
.90
1.00
1.10
1.20
1.30
1.40
1.50
1.60
1.70
1.80
non-dimensional time t
CONFIDENTIAL

Figure 11.

SUMMARY OF FORMULAS

1. Scaling factors (for T. N. T.):

$$L = 13.2 \left(\frac{W}{D}\right)^{1/3} \text{ ft.}$$

$$C = 2.85 \frac{W^{1/3}}{D_o^{5/6}} \text{ sec.}$$

where W = weight of T. N. T. in lbs., D_o = distance, in feet, of the explosion from a point 33 ft. above sea level.

2. Period of pulsation:

$$\bar{T} = 1.47C = 4.19 \frac{W^{1/3}}{D_o^{5/6}} \text{ sec.}$$

in the absence of outside influences; if the bubble is at a distance b_o from a rigid wall, this is to be multiplied by

$$\left(1 + \frac{.185}{b_o}\right)$$

3. Maximum radius:

If the internal energy of the gas is neglected, the maximum radius of the bubble is L. If the internal energy is allowed for, the maximum radius is $a_1 L$, where a_1 is the largest root of $a^3 + \frac{k}{a^{3/4}} = 1$, and k is given by the formula $k = .0607\ D_o^{1/4}$.

4. Non-dimensional momentum at time of minimum size:

The momentum due to gravity and a rigid bottom is

$$\bar{s} = \frac{1}{b_o^2}\left(.113 - \frac{.019}{b_o}\right) + \frac{1}{d-b_o}\left(.704 + \frac{.148}{b_o}\right) .$$

5. Peak pressure for the secondary pulse:

The peak pressure is

$$176\ \frac{W^{1/3}}{R}\ q \text{ atmospheres}$$

where R is the distance in feet from the center of the bubble and q is a factor whose graph is drawn in figure 6.

BIBLIOGRAPHY

[1] G. E. Hudson - "Early and Ultimate Damage due to an Underwater Explosion against 10-inch Diaphragms". Taylor Model Basin Report 509, Aug. 1943.

[2] D. E. J. Offord - "Notes on Damage to British Warships which is of interest in connection with the Study of Bubble Phenomena from Underwater Explosions". Admiralty Naval Construction Dept., WA-669-7, Undex 23, May 1943.

[3] G. I. Taylor - "Vertical Motion of a Spherical Bubble and the Pressure Surrounding It". Taylor Model Basin Report 510, Feb. 1943.

[4] C. Herring - "Theory of the Pulsations of the Gas Bubble Produced by an Underwater Explosion". Division C, NDRC Report C4-sr20-010, OSRD 236, Oct. 1941.

[5] M. Shiffman - "The Effect of a Rigid Wall on the Motion of an Underwater Gas Bubble". AMP Memo 37.1; AMG-NYU, No. 7, July 1943.

[6] E. H. Kennard - "Migration of Underwater Gas Globes due to Gravity and Neighboring Surfaces". Taylor Model Basin Report R-182, Dec. 1943.

[7] J. G. Kirkwood - "Memorandum on the Plastic Deformation of Marine Structures by an Underwater Explosion Wave". OSRD No. 788, Aug. 1942.

[8] M. Shiffman - "The Effect of Non-Spherical Shape on the Motion of a Rising Underwater Bubble". AMP Memo 37.5; AMG-NYU, No. 23, Sept. 1943.

[9] H. F. Willis and M. I. Willis - "Underwater Explosions Near the Sea-Bed". HMA/SEE Internal Report No. 142; OSRD No. WA-1078-4, Sept. 1943.

N. Y. U. Institute of
Mathematical Sciences
25 Waverly Place
New York 3, N. Y.